Vortex dynamics in high Froude number variable-density flows

Laurent Joly

J.N. Reinaud, J. Micallef, J. Suarez, L. Bretonnet,
J. Fontane, G. Campagne

ENSICA - Département de Mécanique des Fluides
Toulouse - France

University of Alberta – Mech.Eng. Dep. – Seminar on December the 2nd – 2004

Outline of the talk

1. Introduction - Illustrative examples from experiments and simulations
2. The baroclinic torque in high Froude number flows, its organization, scale and order of magnitude
3. Transition of the inhomogeneous mixing-layer and the 2D secondary baroclinic instability
4. The strain field of 2D light jets and the question of side-jets
5. Mass segregation in 2D turbulence and the baroclinic instability of massive vortices

Stratified medium in a gravity field

Tilted tank experiments : « A method of producing a shear flow in a stratified fluid » S.A. Thorpe JFM32 1968

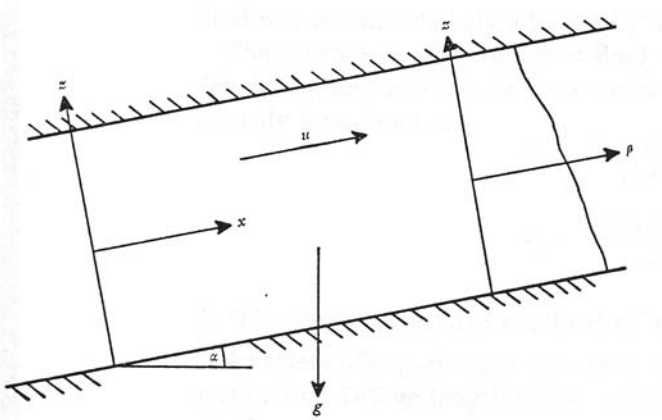

FIGURE 1. Notation.

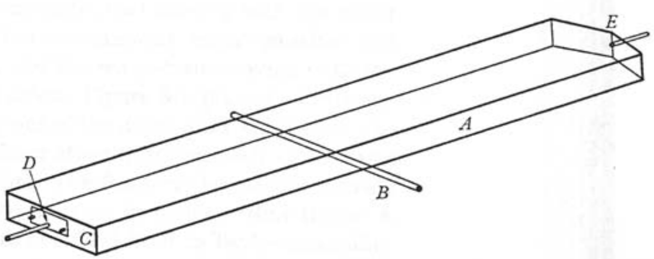

FIGURE 2. The apparatus.

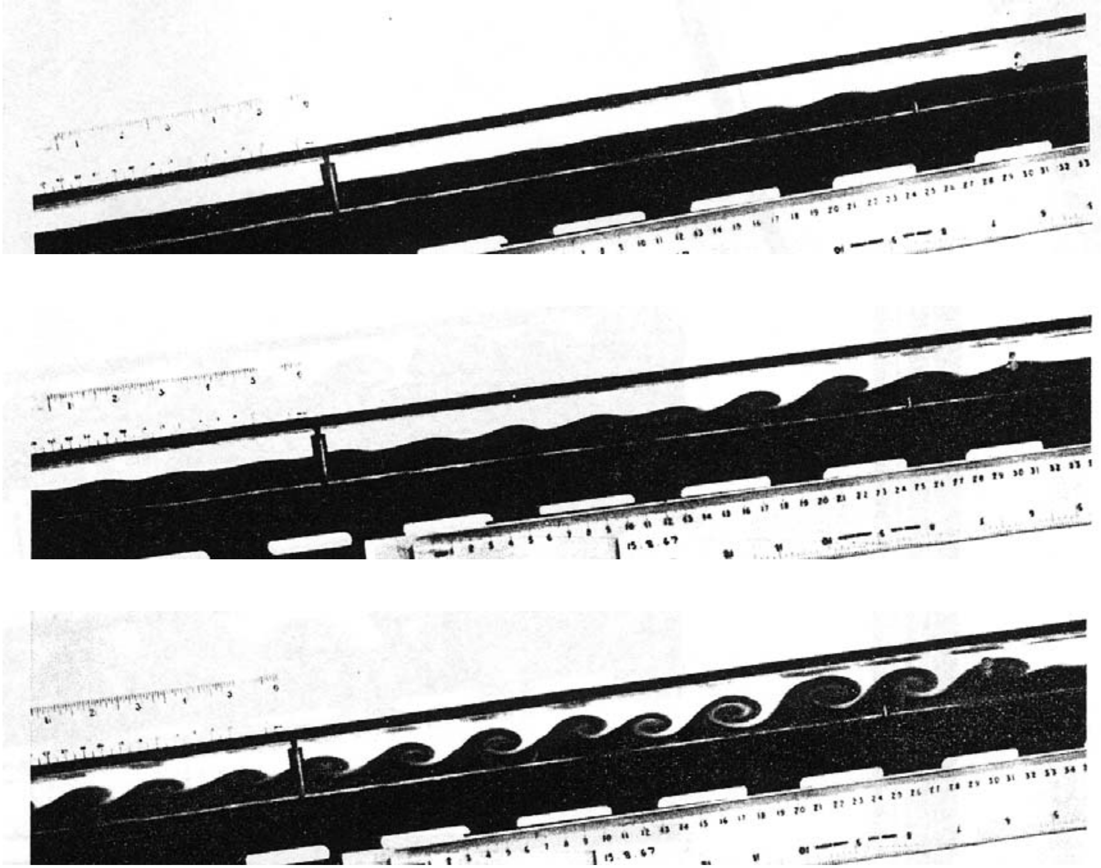

Two-dimensionnal Stratified Mixing Layer (vertical shear)

Klaassen and Peltier JFM227 (1991)

Re=300

$$Ri = g\frac{\Delta\rho}{\bar{\rho}}\frac{\delta_\omega}{\Delta U^2} = \frac{1}{Fr^2}$$

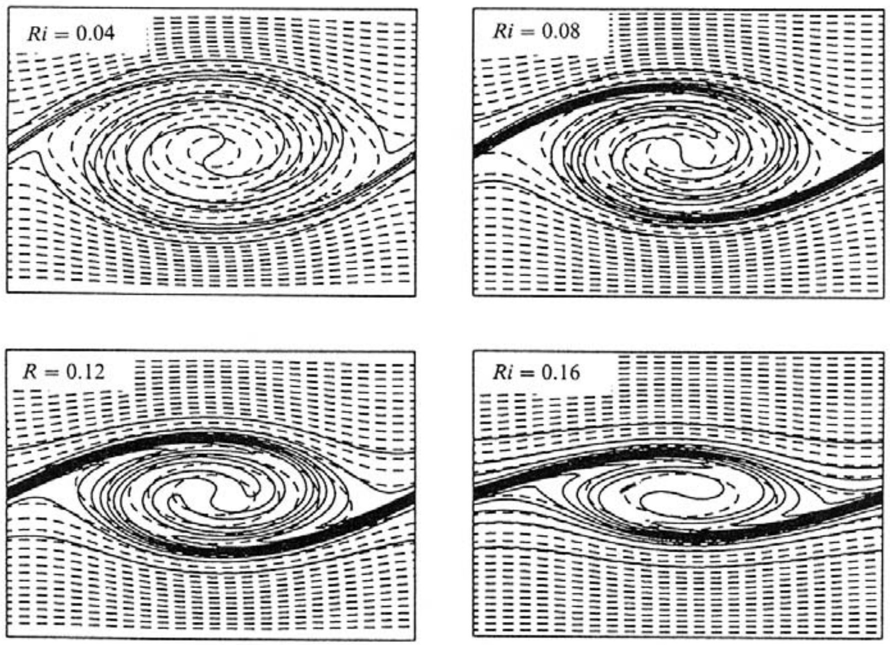

FIGURE 2. Stream function (dashed contours) and potential temperature field (solid contours) for stratified Kelvin–Helmholtz billows at various Richardson numbers Ri and $Re = 300$, $Pr = 1$. The waves are shown at the times of maximum kinetic energy, which are $t = 26$ ($Ri = 0$), 30 ($Ri = 0.04$), 34 ($Ri = 0.08$), 42 ($Ri = 0.12$) and 52 ($Ri = 0.16$). Contour intervals are the same for each wave. The horizontal period is $14h$ and the domain height is $10h$.

Staquet JFM296 (1995)

Re=2000 – Ri = 0.167

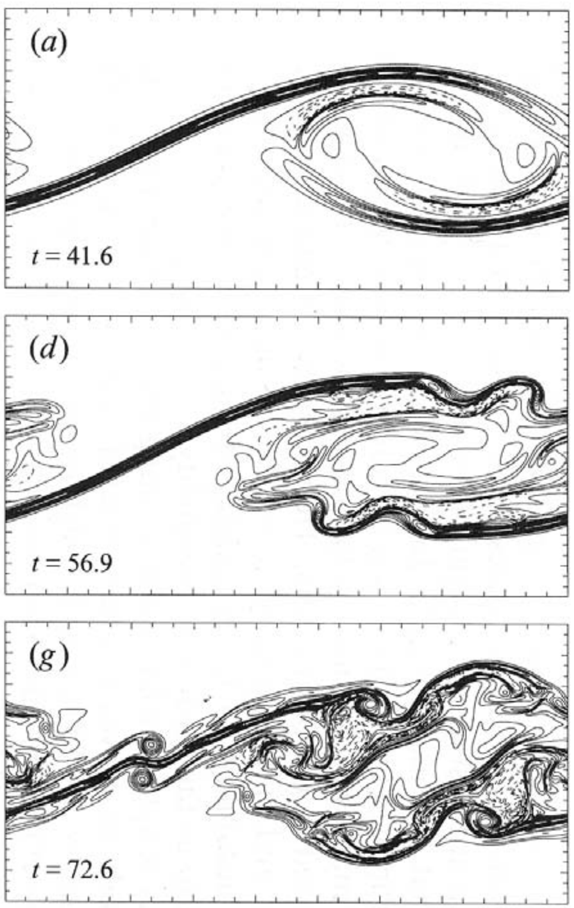

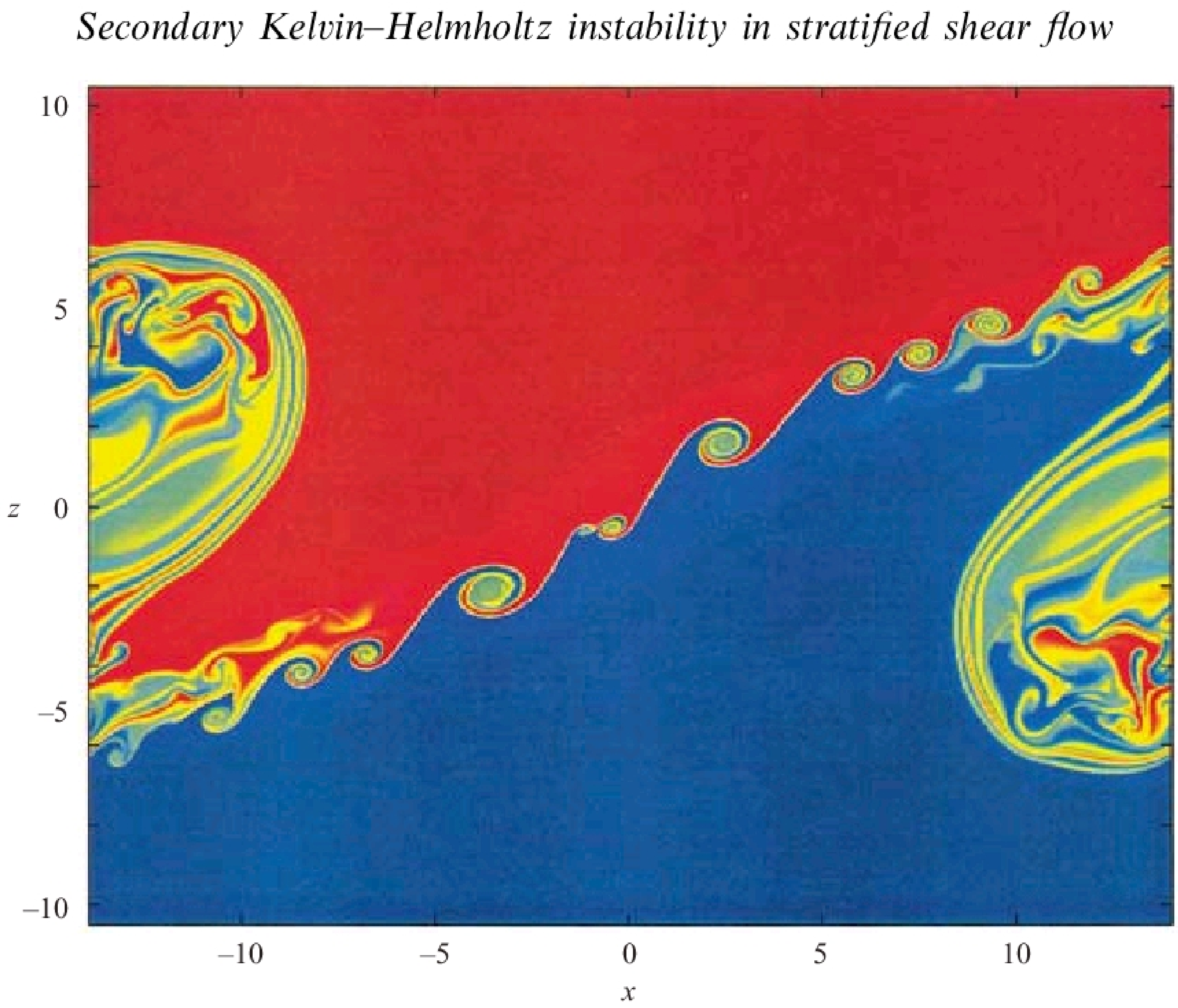
Secondary Kelvin–Helmholtz instability in stratified shear flow
10
5
z
0
–5
–10
–10
–5
0
5
10
x

Three-dimensionnal stratified Mixing Layer

Schowalter, Van Atta and Lasheras JFM281 (1994)

Ri=0.06

Klaassen and Peltier JFM227 (1991)

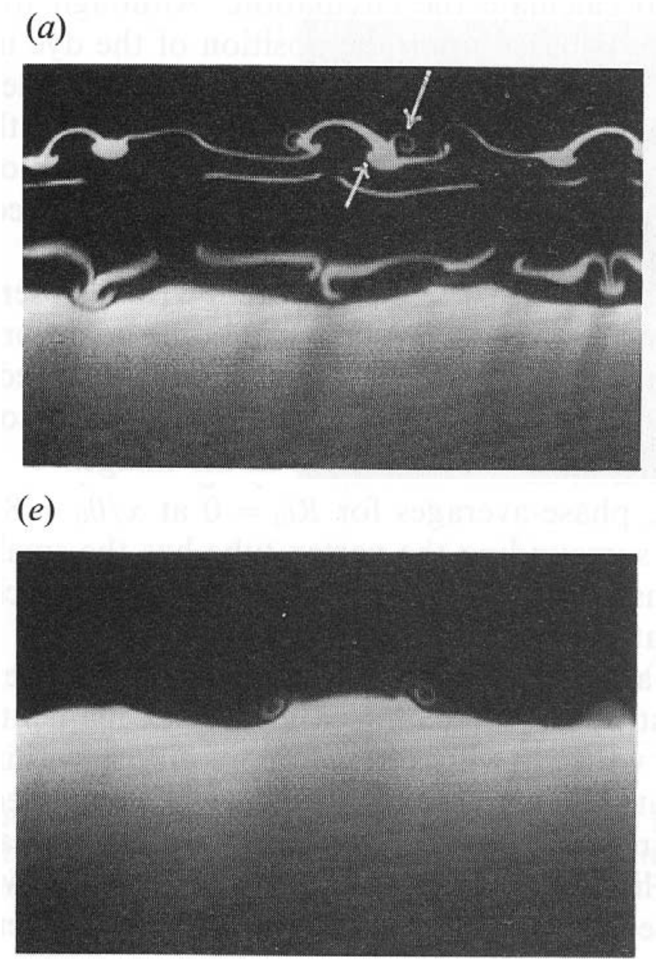

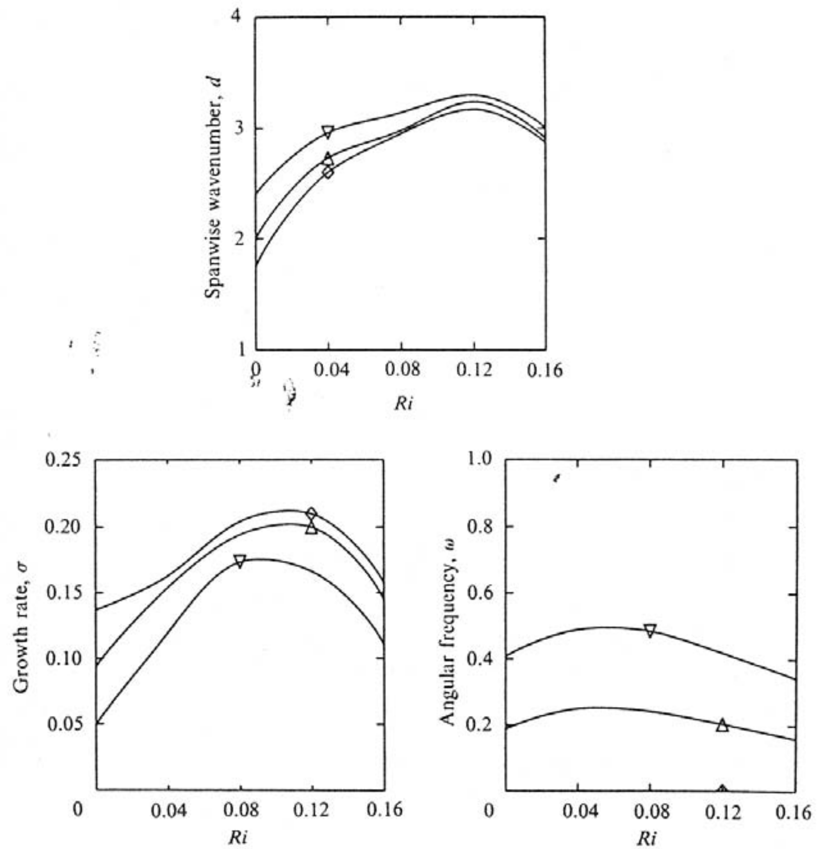

FIGURE 22. The effect of bulk Richardson number Ri on the most unstable ω_0 ($\Diamond$), Ω_1 ($\triangle$), and ω_2 (∇) modes of the maximum amplitude KH wave state. For Floquet parameter $b = 0$.

Brown and Roshko, « On density effects and large structure in turbulent mixing layers », JFM 64, 1974

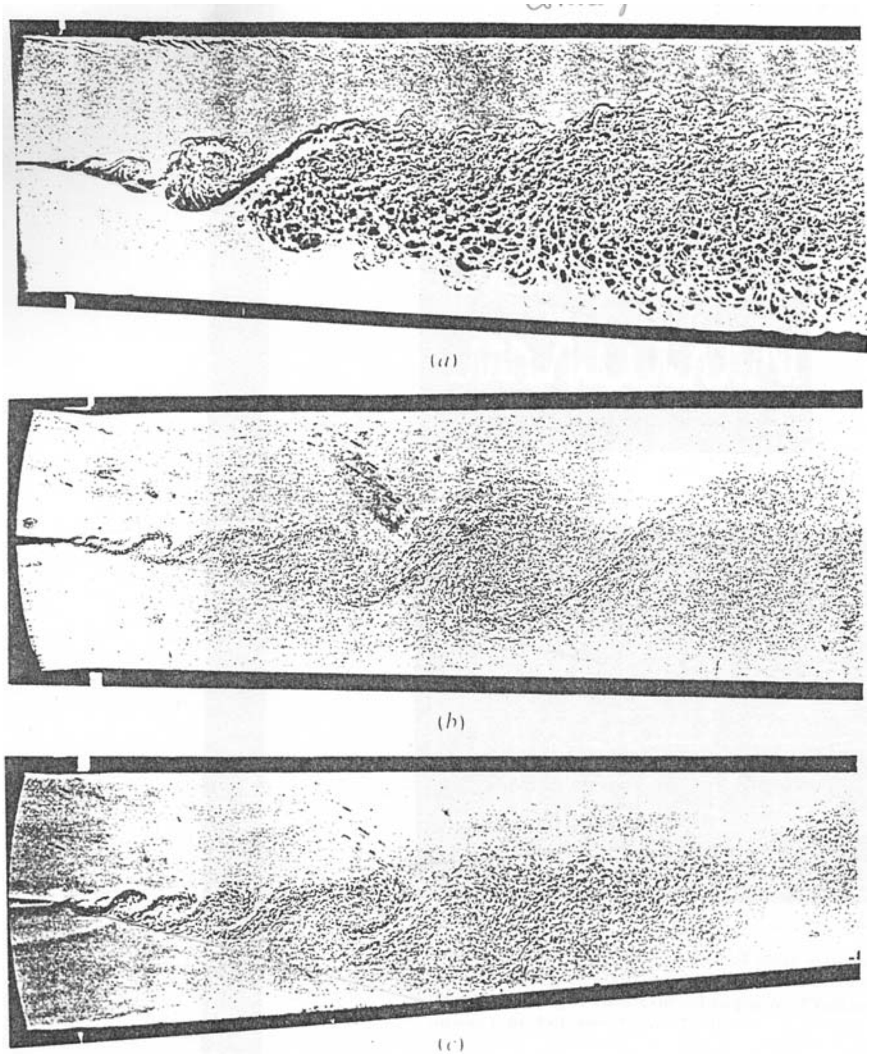

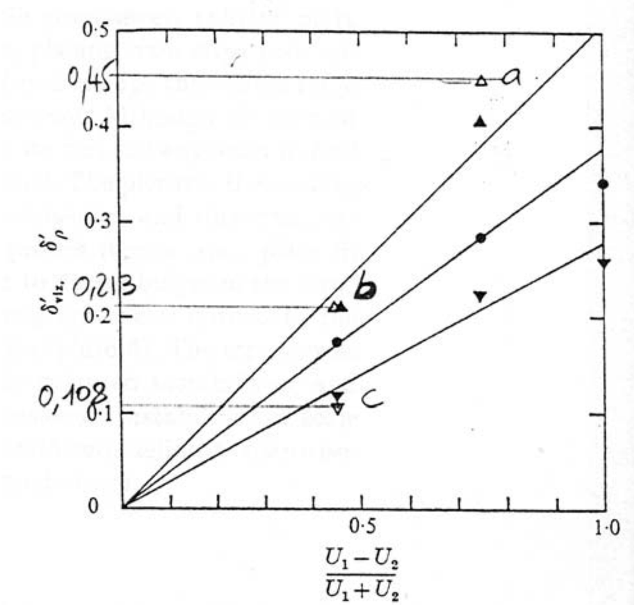

FIGURE 7. Visual growth rates.

δ'_{ρ}	δ'_{viz}	ρ_2/ρ_1
△	▲	7
	●	1
▽	▼	$\frac{1}{7}$

Two-dimensionnal secondary baroclinic instability : Reinaud, Joly and Chassaing, PoF vol 12(10), pp 2489-2505, 2000

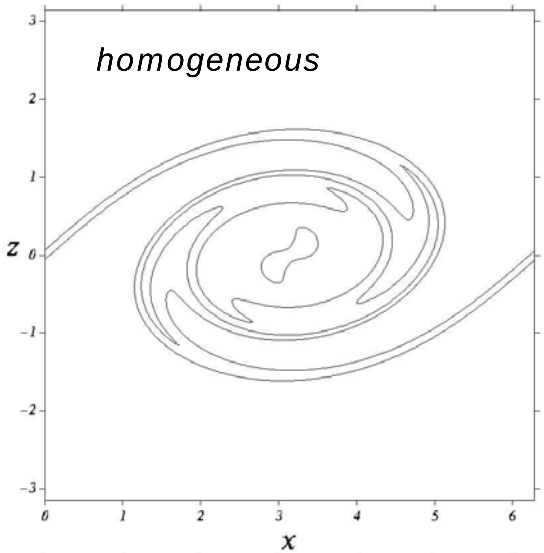

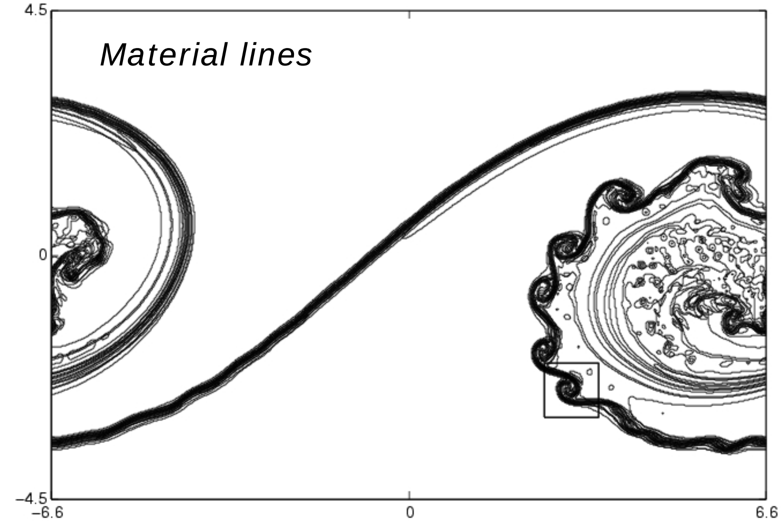

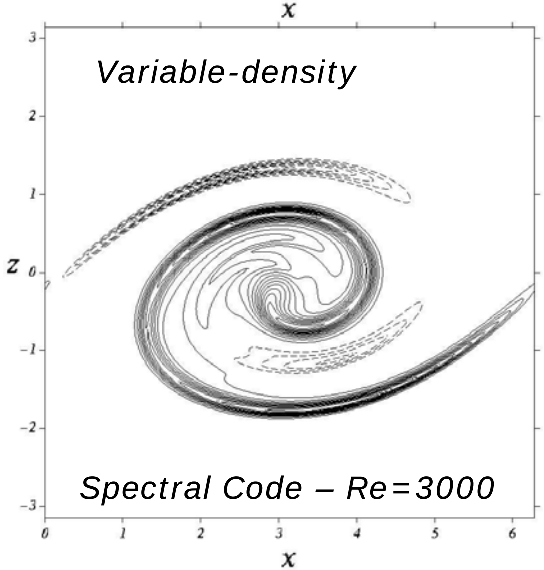

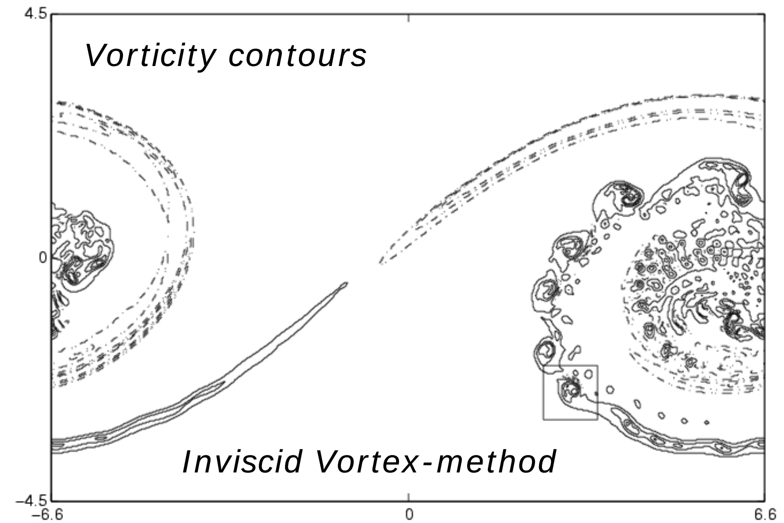

Self-excited oscillations and mixing in a hot jet : Monkewitz and Bechert, PoF Gallery of fluid motion, 1988

S=0,47

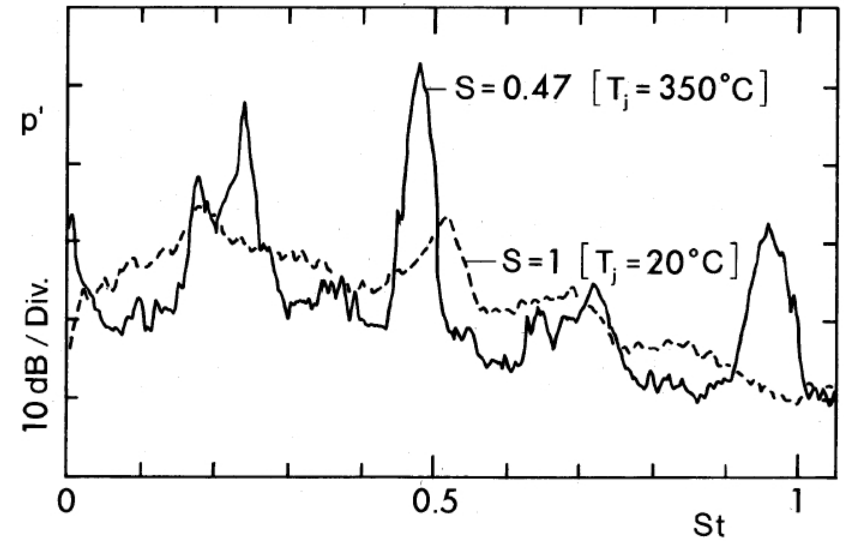

Figure 3. Pressure spectra (B&K $\frac{1}{4}$ in. microphone located at $x/D = 0.2$, $r/D = 1$) for the hot jet of Fig. 2 and a cold jet of equal dynamic head $q = 135$ Pa.

1. Introduction - Illustrative examples from experiments and simulations

non-barotropic flows exhibit deviations from their homogeneous or barotropic equivalent

2. The baroclinic torque in high Froude number flows, its nature, order of magnitude and organization
3. Transition of the inhomogeneous mixing-layer and the 2D secondary baroclinic instability
4. The strain field of 2D light jets and the question of side-jets
5. Mass segregation in 2D turbulence and the baroclinic instability of massive vortices

Focus : Incompressible mixing at infinite Froude numbers

$$\mathrm{d}_t \varrho = a\Delta\varrho = -d \qquad \varrho = \ln\rho\ , \quad d = \boldsymbol{\nabla}\cdot\mathbf{u}$$

$$\mathrm{d}_t \mathbf{u} = -\boldsymbol{\nabla}\pi - \pi\boldsymbol{\nabla}\varrho + \nu\Delta\mathbf{u} \qquad \pi = p/\rho$$

$$\mathrm{d}_t \boldsymbol{\omega} = (\boldsymbol{\omega}\cdot\boldsymbol{\nabla})\mathbf{u} - d\,\boldsymbol{\omega} - \boldsymbol{\nabla}\pi\times\boldsymbol{\nabla}\varrho + \nu\Delta\boldsymbol{\omega}$$

$$\frac{\mathrm{d}\boldsymbol{\omega}}{\mathrm{d}t} = (\boldsymbol{\omega}\cdot\boldsymbol{\nabla})\mathbf{u} - \frac{1}{\rho^2}\boldsymbol{\nabla}P\times\boldsymbol{\nabla}\rho - d\,\boldsymbol{\omega} + \nu\Delta\boldsymbol{\omega}$$

$$s = \rho_2/\rho_1$$

$$C_\rho = \frac{\rho_2 - \rho_1}{\rho_2 + \rho_1}$$

$$C_\rho = (s-1)/(1+s)$$

Condition : $2\rho_m - \Delta\rho > 0$

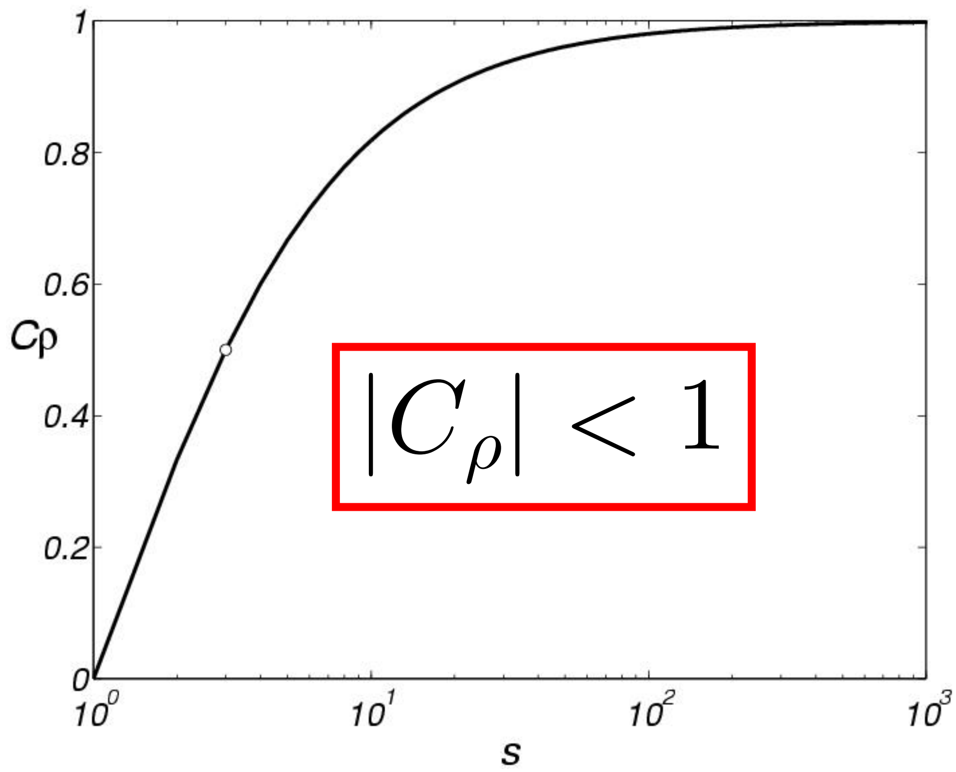

$$\mathrm{d}_t\varrho = \frac{1}{ReSc}\Delta\varrho = -\frac{1}{C_\rho}d$$

$$\mathrm{d}_t\mathbf{u} = -\boldsymbol{\nabla}\pi - \underline{C_\rho\pi\boldsymbol{\nabla}\varrho} + \frac{1}{Re}\Delta\mathbf{u}$$

$$\mathrm{d}_t\boldsymbol{\omega} = \underline{(\boldsymbol{\omega}\cdot\boldsymbol{\nabla})\mathbf{u}} - d\,\boldsymbol{\omega} - \underline{\boldsymbol{\nabla}\pi\times\boldsymbol{\nabla}\varrho} + \nu\Delta\boldsymbol{\omega}$$

Vs $\quad (\boldsymbol{\omega}\cdot\boldsymbol{\nabla})\mathbf{u} \sim \mathcal{O}(\frac{u^2}{\lambda^2})$

Ba $\quad \boldsymbol{\nabla}\pi\times\boldsymbol{\nabla}\varrho \sim \mathcal{O}(\frac{u^2}{\ell}\,\frac{C_\rho}{\lambda_\rho})$

$$\boxed{\frac{\mathrm{Ba}}{\mathrm{Vs}} \sim C_\rho\cdot\frac{\lambda}{\lambda_\rho}\cdot\frac{\lambda}{\ell}}$$

$$\frac{\mathrm{Ba}}{\mathrm{Vs}} \sim \; C_\rho \cdot \frac{\lambda}{\lambda_\rho} \cdot \frac{\lambda}{\ell}$$

- Fully developped 3D turbulence $$\frac{\mathrm{Ba}}{\mathrm{Vs}} \sim \; \frac{\lambda}{\lambda_\rho} \cdot \frac{C_\rho}{Re_\lambda}$$

Vortex stretching much larger than baroclinic torque in high Reynolds number turbulence

- Two-dimensional flows : no vortex stretching $\boldsymbol{\omega} \perp \boldsymbol{\nabla} \mathbf{u}$

No vortex stretching, baroclinic torque only source/sink of vorticity

- Transition flows $$\frac{\lambda}{\ell} \sim \mathcal{O}(1)$$

The baroclinic torque may bias the transition

Kelvin-Helmholtz instability s=3, Re = $U\delta/\nu$ = 1500

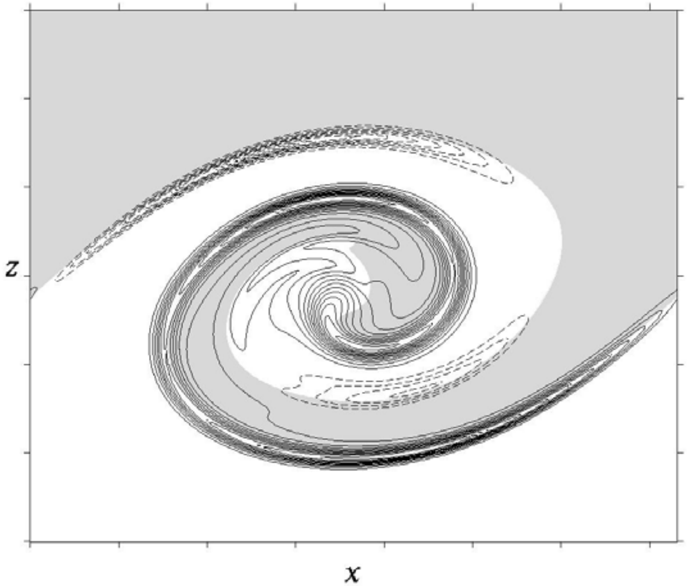

t=12

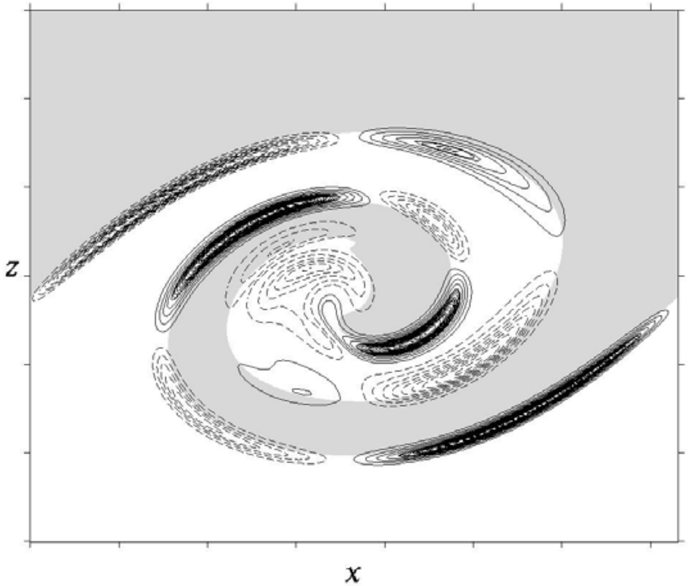

Vorticity

Baroclinic torque

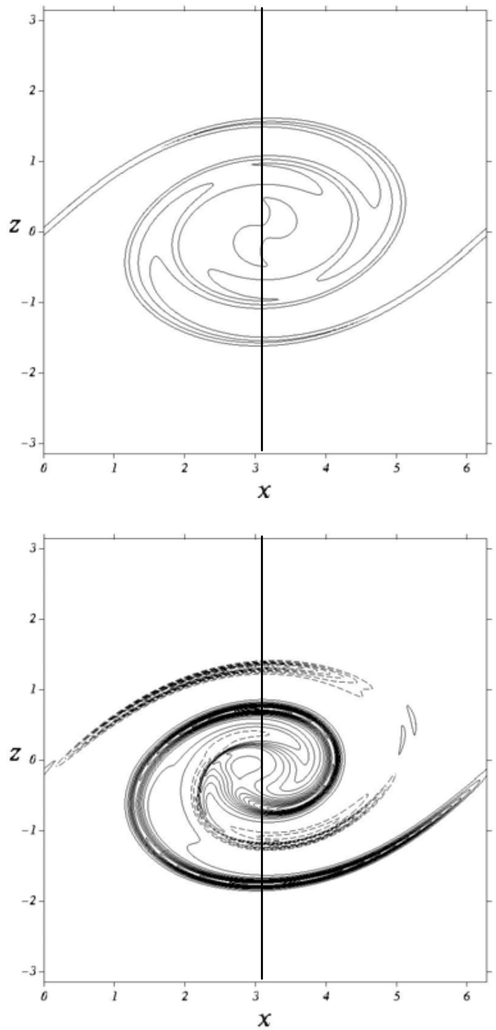

Mixing layer s = 1 or 3 , Re = 3000, t=12

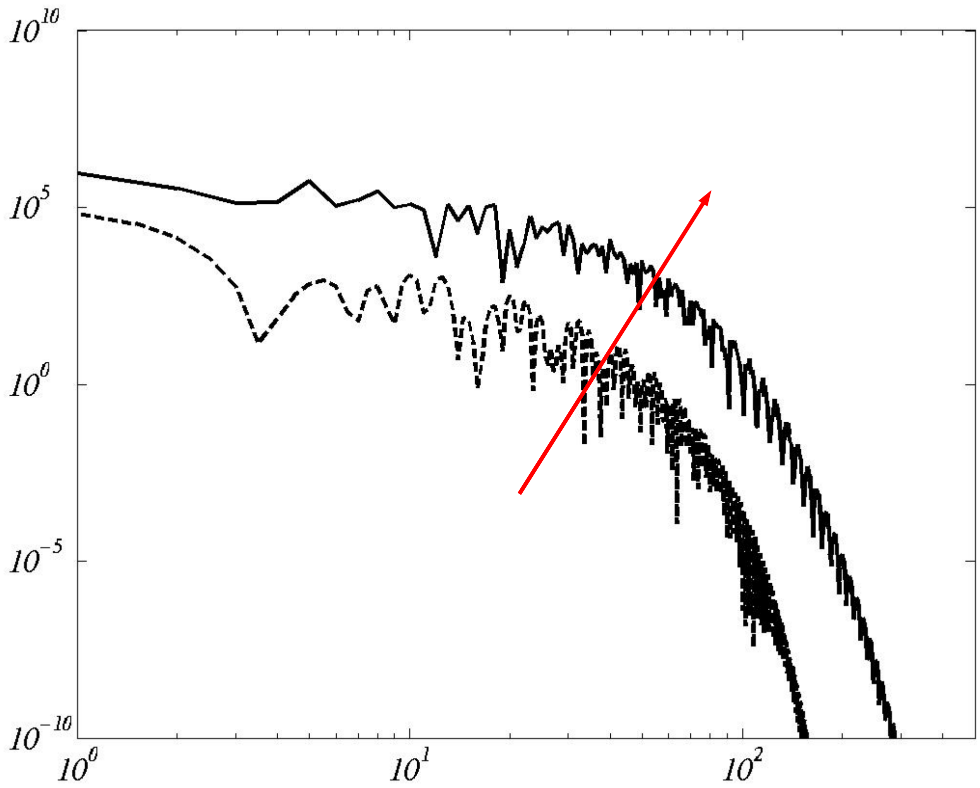

Temporal mixing layer s=3, Re = Uδ/ν = 500,1500,3000

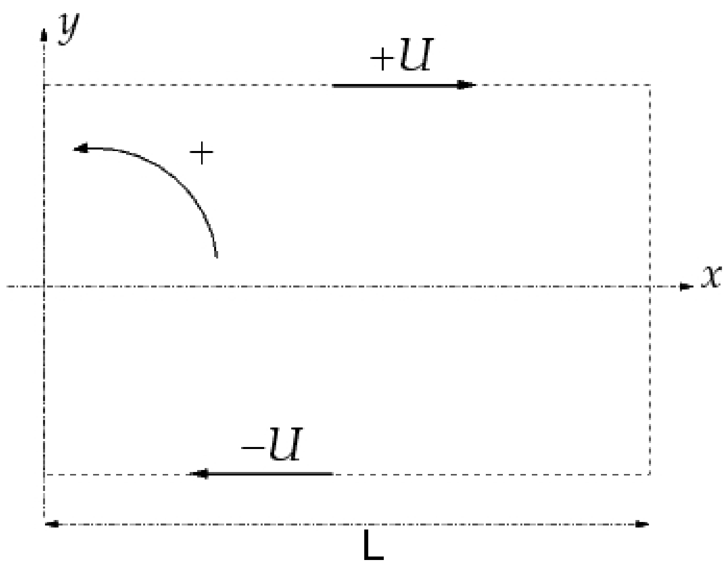

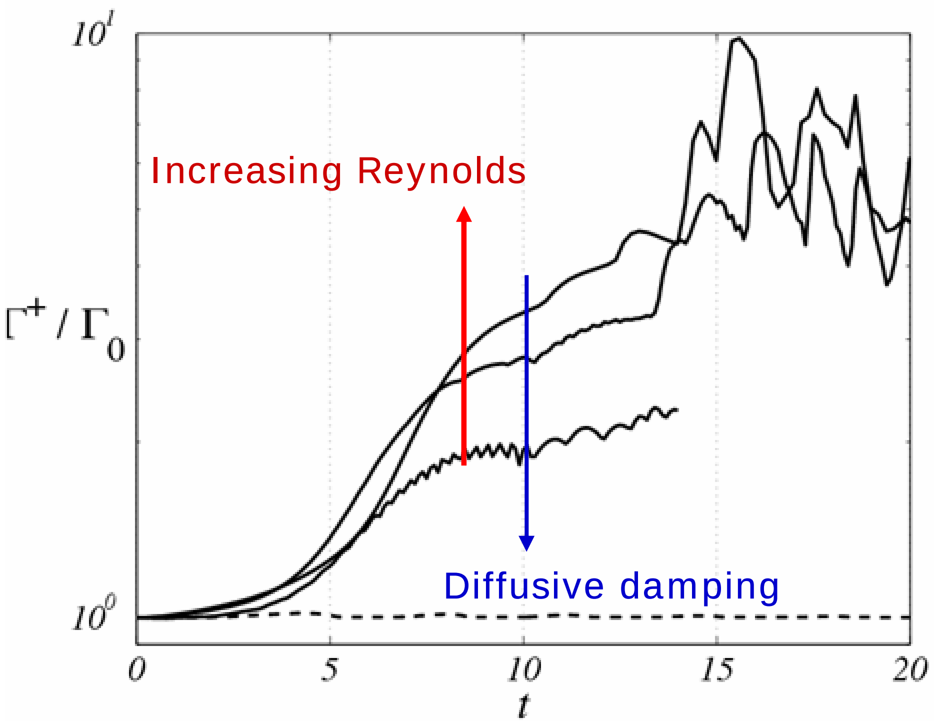

$$\Gamma_0 = -2UL$$

$$\Gamma^+ = \int_{\text{period}} (\omega < 0)\mathrm{d}\sigma$$

Outline of the talk

1. *Introduction*
2. *The baroclinic torque*

- *Scales with the bounded density contrast*
- *Inertial nature : accelerated inhomogeneous medium*
- *Competes with vortex stretching in transition flows and 2D flows*
- *Enstrophy source at high wavenumbers/small scales*
- *Intense local source/sink of vorticity but a weak net effect*
- *Significantly damped by diffusion, enhanced by isopycnal stretching*

3. *Transition of the inhomogeneous mixing-layer and the 2D secondary baroclinic instability*

Normalized vorticity along the central material line

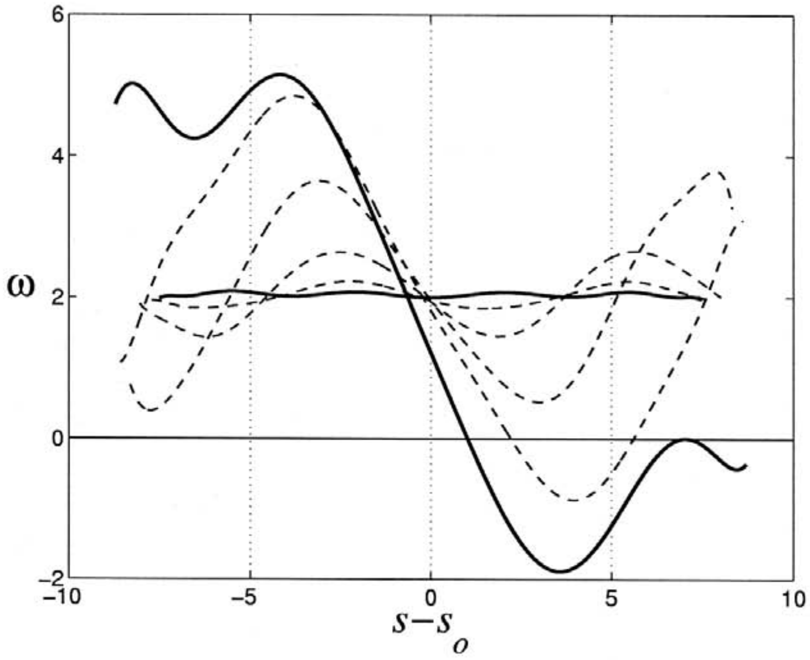

Figure 3.3: Normalized vorticity $\omega \times \tau$ along the central material line (where $\rho = (\rho_{\text{upper}} + \rho_{\text{lower}})/2$) of the variable density mixing layer with $Re = 1500$ and density ratio $S_\rho = 3$. The solid curves are the initial vorticity level and the one at t=10. Dashed lines are every $\Delta t = 2$ and the dot-dashed line marks the zero threshold. The abscissa is given along the normalized curvilinear coordinate s/δ^0_ω associated to the material line, s_o being the origin at the saddle point.

The stretched density-gradient and vorticity filament,

Reinaud, Joly et Chassaing, Physics of Fluids (2002)

$$\mathbf{u} = (\gamma x, -\gamma y) \qquad \mathbf{g} = (0, g_y)$$

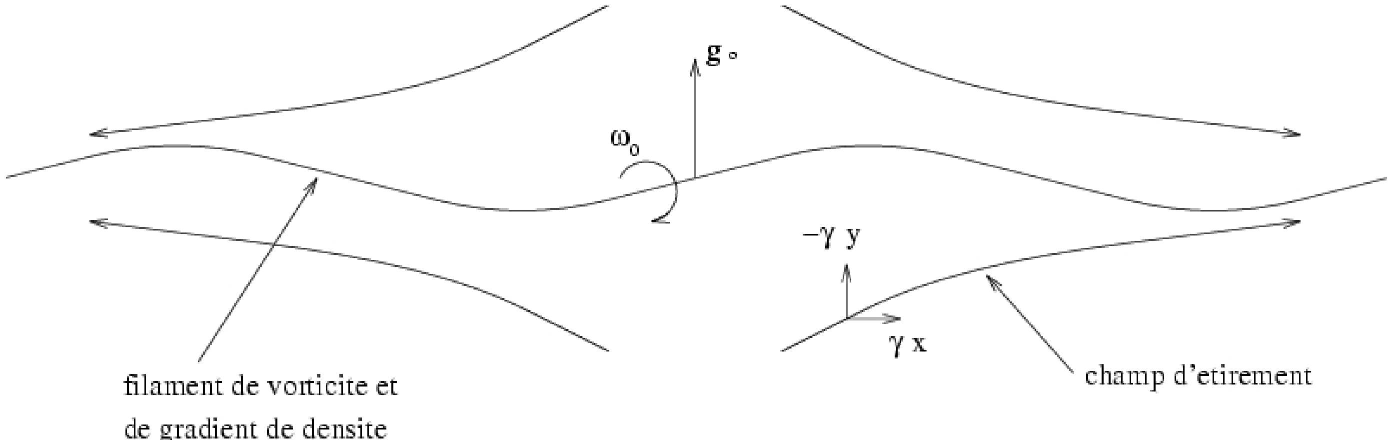

$$\mathrm{d}_t g_y = \gamma g_y \quad \rightarrow \quad g_y(x,t) = g_0 \exp(\gamma t)$$

$$\mathrm{d}_t \omega = \mathrm{d}_t u \frac{g_y}{\rho_0} = \gamma^2 x \frac{g_0}{\rho_0} \exp(\gamma t) \quad \rightarrow \quad \omega(x,t) = \gamma x \frac{g_0}{\rho_0} \sinh(\gamma t) + \omega_0$$

$$\frac{\omega(x,t)}{\gamma} = -\frac{g_0}{\rho_0} x \sinh(\gamma t) + \frac{\omega_0}{\gamma}$$

Density

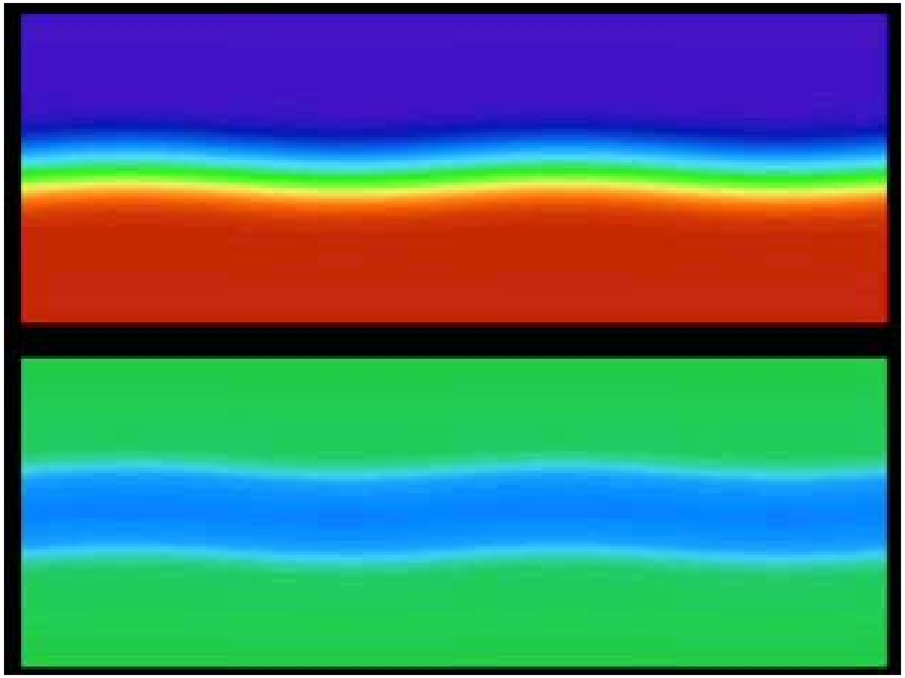

High-density fluid

Low-density fluid

Vorticity

The secondary instability : scale invariance ?

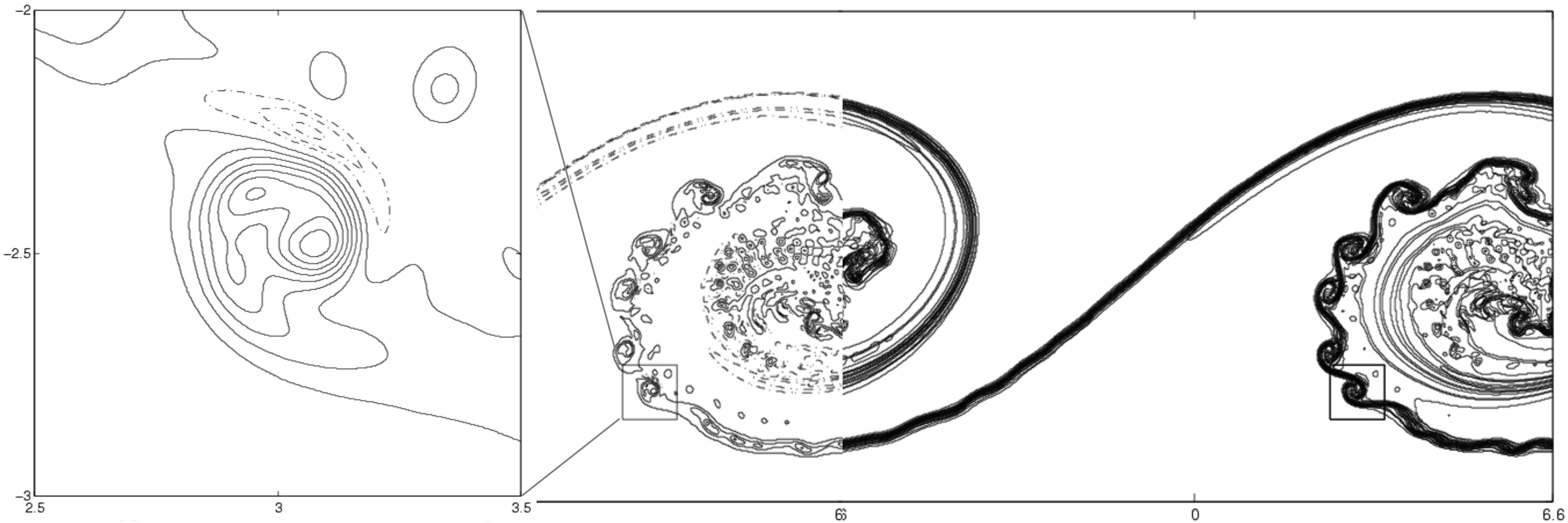

- A specific transition mecanism of the inhomogeneous shear flow;
- Twodimensional secondary mode;
- The vorticity pattern is repeated in second generation structures, and so on untill viscous length scales are produced and baroclinic vorticity generation is prevented.

Forced spatially developing mixing-layer (simulations with a variable density vortex method)

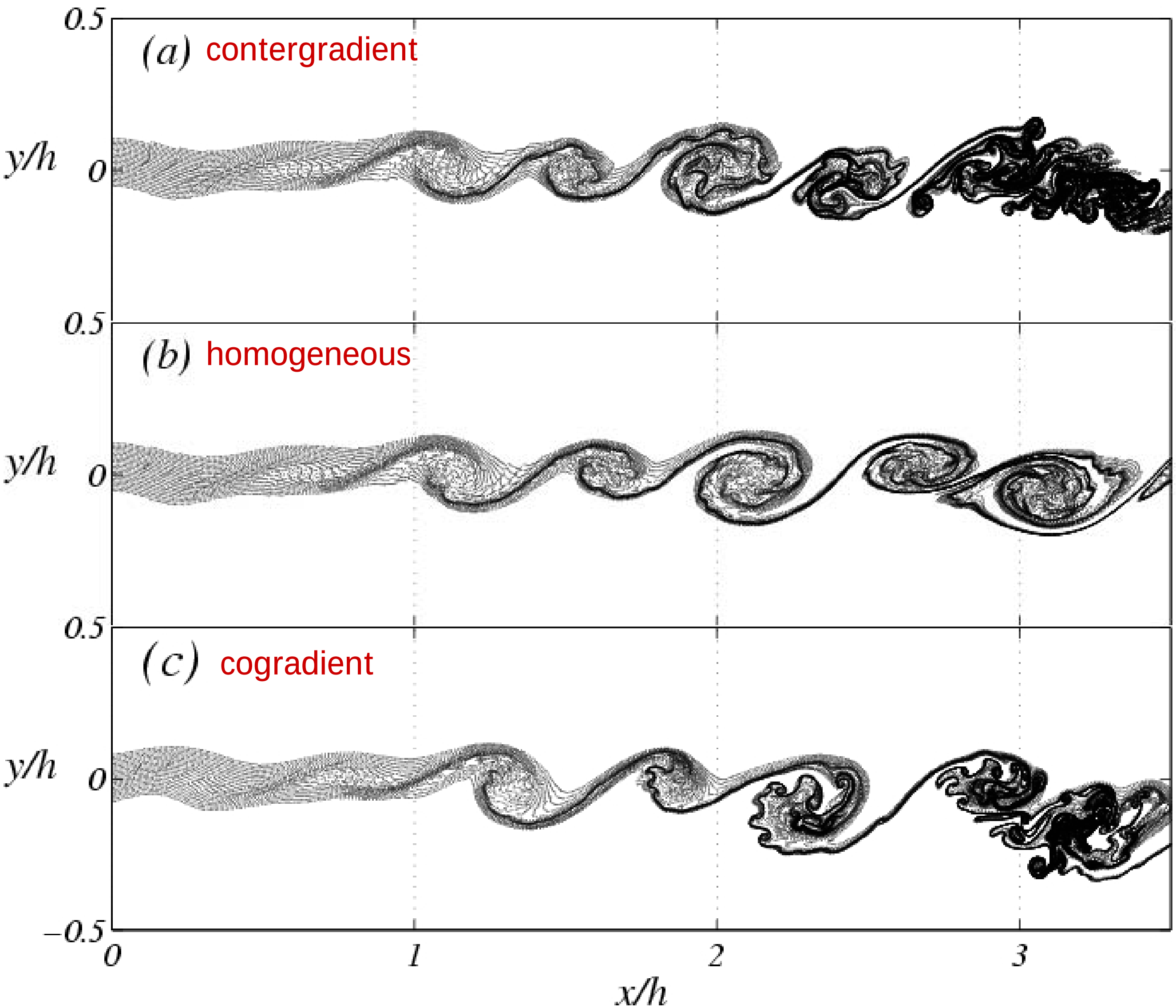

3. *The 2D mixing-layer in the nonlinear regime and the secondary baroclinic instability*

- *The non-linear stage ends in a rather asymmetric vorticity distribution due to alternate positive and negative baroclinic contributions;*
- *From the vorticity field the structure is not a standard KH smooth roller;*
- *A secondary baroclinic instability developes on the light side of the KH billow;*
- *Not observed so far at Reynolds numbers up to 3000 nor in experimental realizations of high Reynolds number flows;*
- *Provides a 2D bypass route to turbulence under high Reynolds number conditions.*

4. *The strain field of 2D light jets and the question of side-jets*
5. *Mass segregation in 2D turbulence and the baroclinic instability of massive vortices*

Sides ejetions in the helium jet : illustration

Transition of the turbulent helium jet

Influence of the Reynolds number

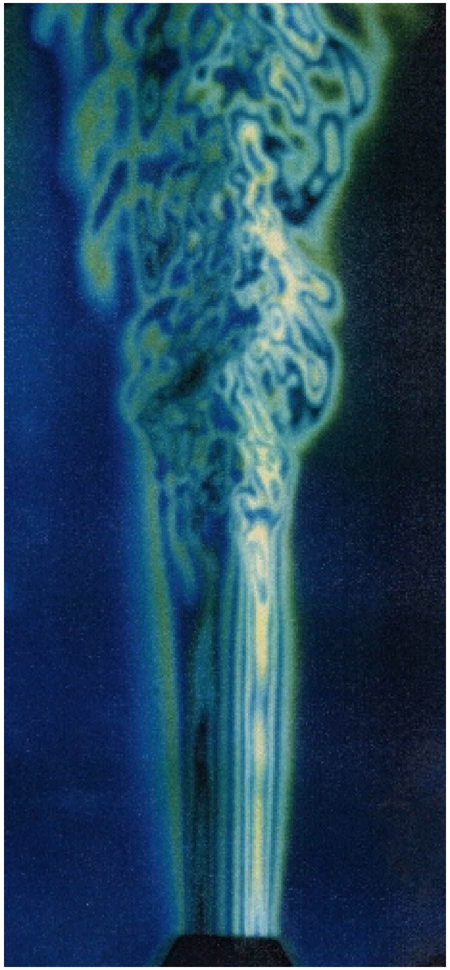

Re = 750

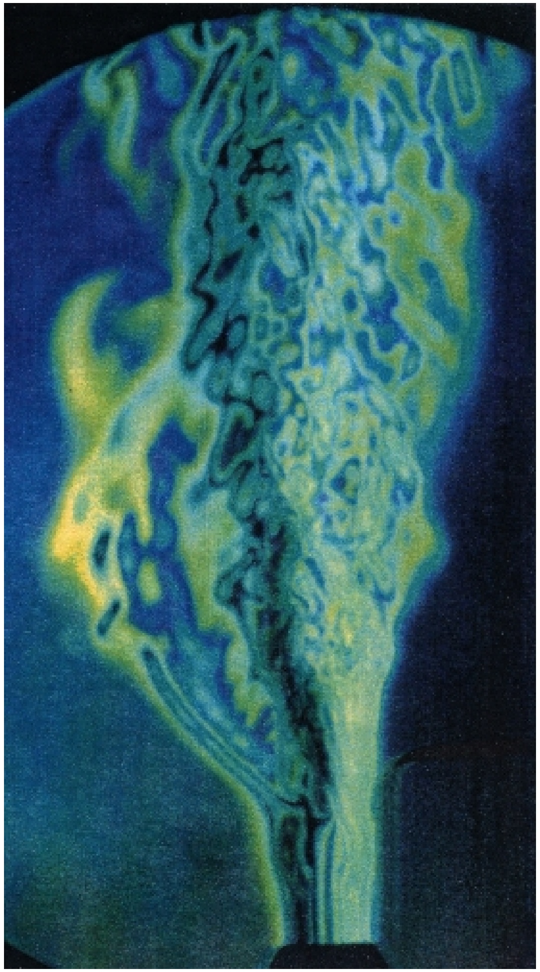

Re = 1000

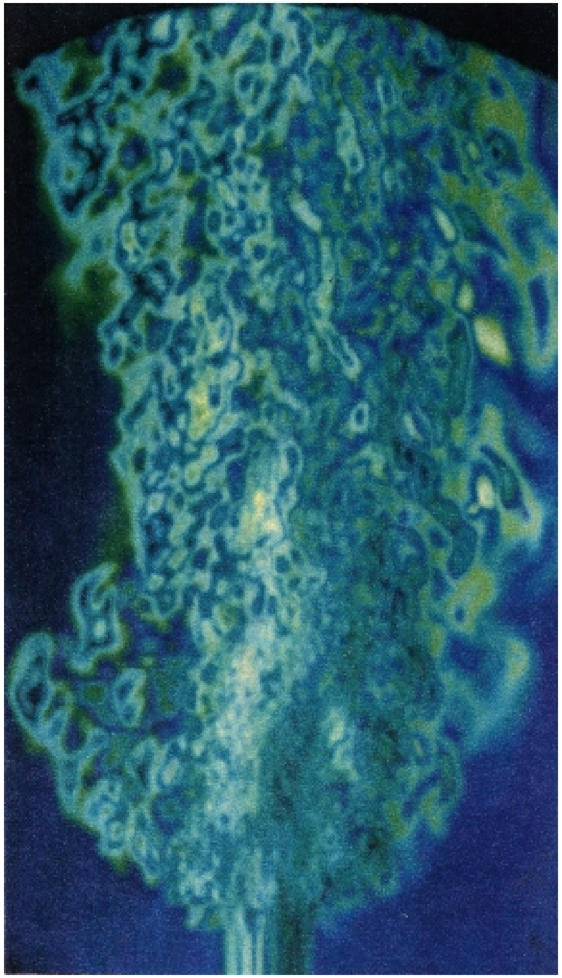

Re = 2600

Paradigm of secondary 3D mode yielding counter-rotative vortices lying between adjacent distorted rings

Side jets induced by pairs of counter-rotative streamwise aligned vortices

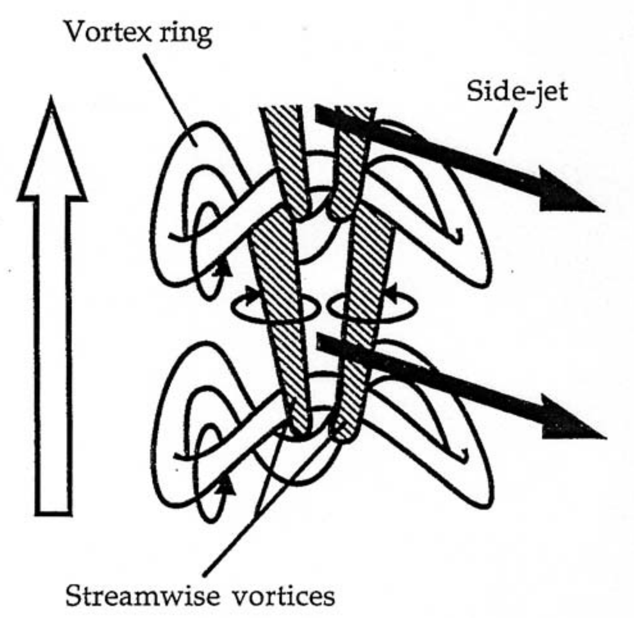

FIG. 6. Vortical structures involved in the side-jet generation process. Only a single streamwise pair is represented (hatched structures) while two consecutive vortex rings are sketched (white structures). The radial ejection of fluid is symbolized by the two black arrows emerging from the streamwise pair.

Brancher, Chomaz & Huerre (1994)

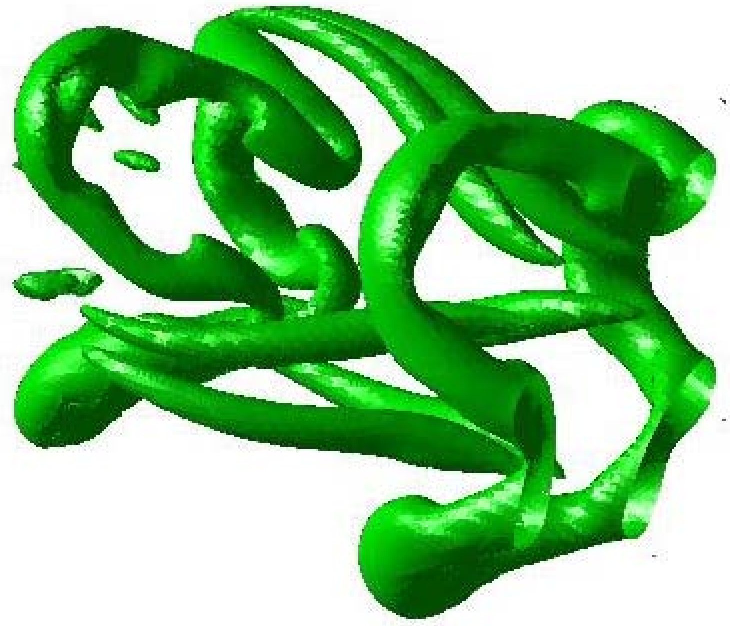

Lambda2 probe of coherent structures in a DNS of a homogeneous 3D temporal jet with a 3-lobe corrugation of the initial vorticity tube.

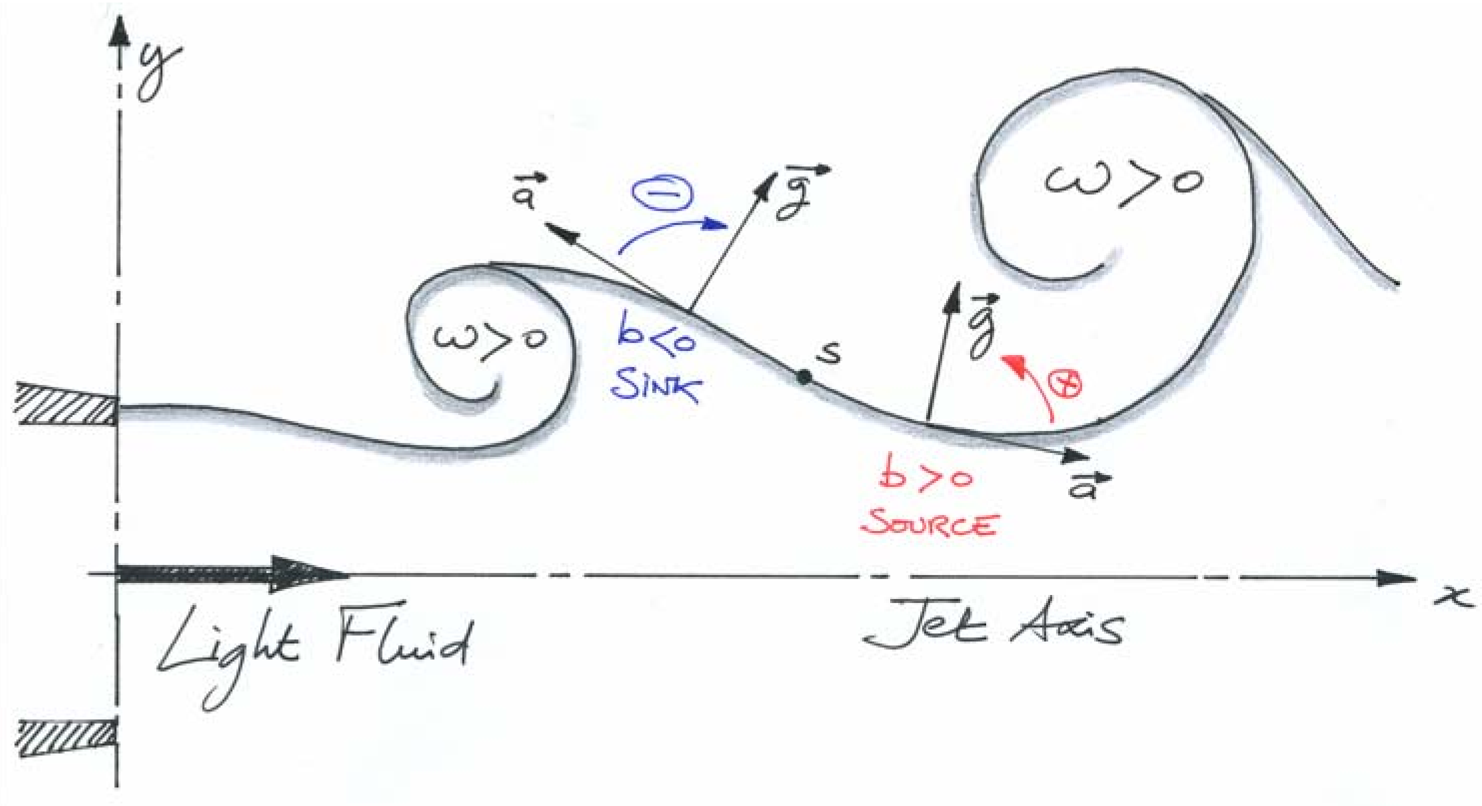
y
ω>0
ω>0
a
g
b<0
SINK
s
g
b>0
SOURCE
a
x
Light Fluid
Jet Axis

The strain rate and the shear rate are measured along some relevant line

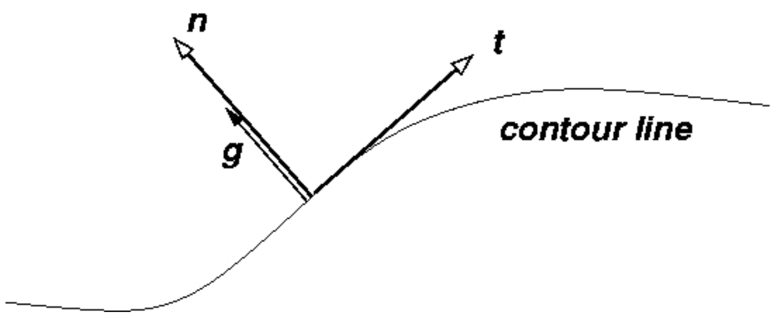

$$\lambda = \frac{\partial u_t}{\partial n} \quad , \quad \gamma = \frac{\partial u_t}{\partial t}$$

$$\lambda = \mathbf{n} \cdot \nabla \mathbf{u} \cdot \mathbf{t} \quad , \quad \gamma = \mathbf{t} \cdot \nabla \mathbf{u} \cdot \mathbf{t}$$

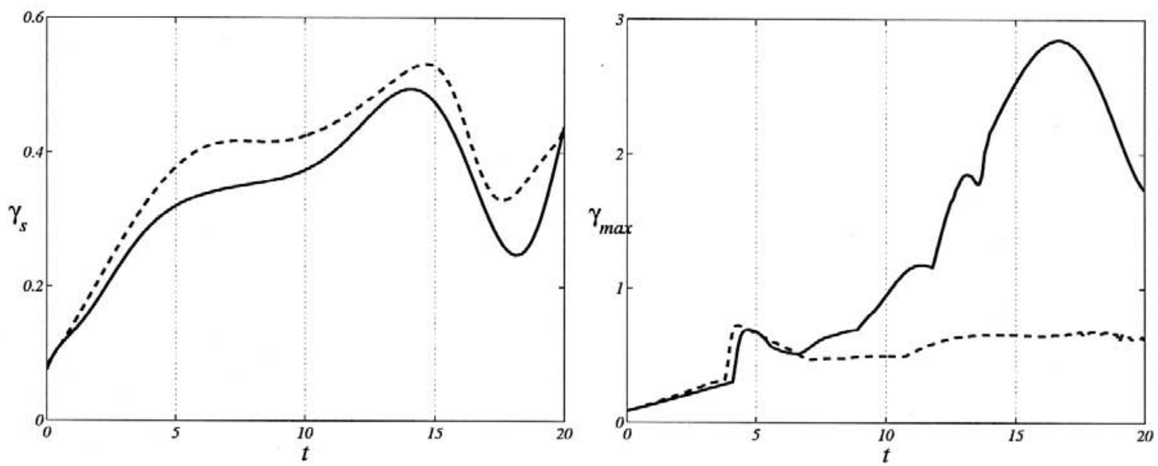

Figure 3.7: Left : the evolution of the strain rate γ_s normal to the density gradient at the saddle point between the main 2D structures. Right : evolution of the overall maximum of the strain rate $\gamma_{\max}$. Solid line : variable density mixing-layer at $S_\rho = 3$; dashed line : passive scalar mixing-layer.

« Variable density fluid turbulence » 2003

Chassaing, Antonia, Anselmet, Joly and Sarkar, Kluwer

The strain field along material lines

Temporal jet s=1/3, Re = UD/ν = 2500

Red : positive γ (***stretching***) – Blue : negative γ (***compression***) – Shaded : above same positive level

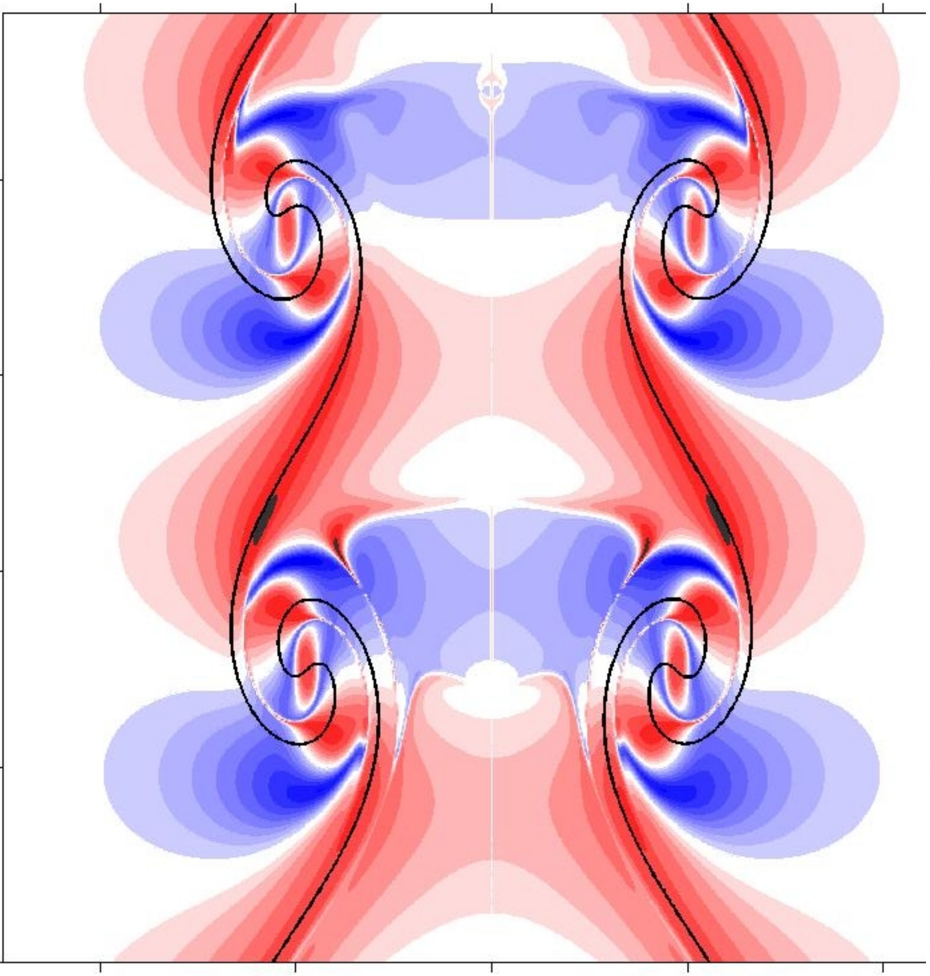

Passive scalar

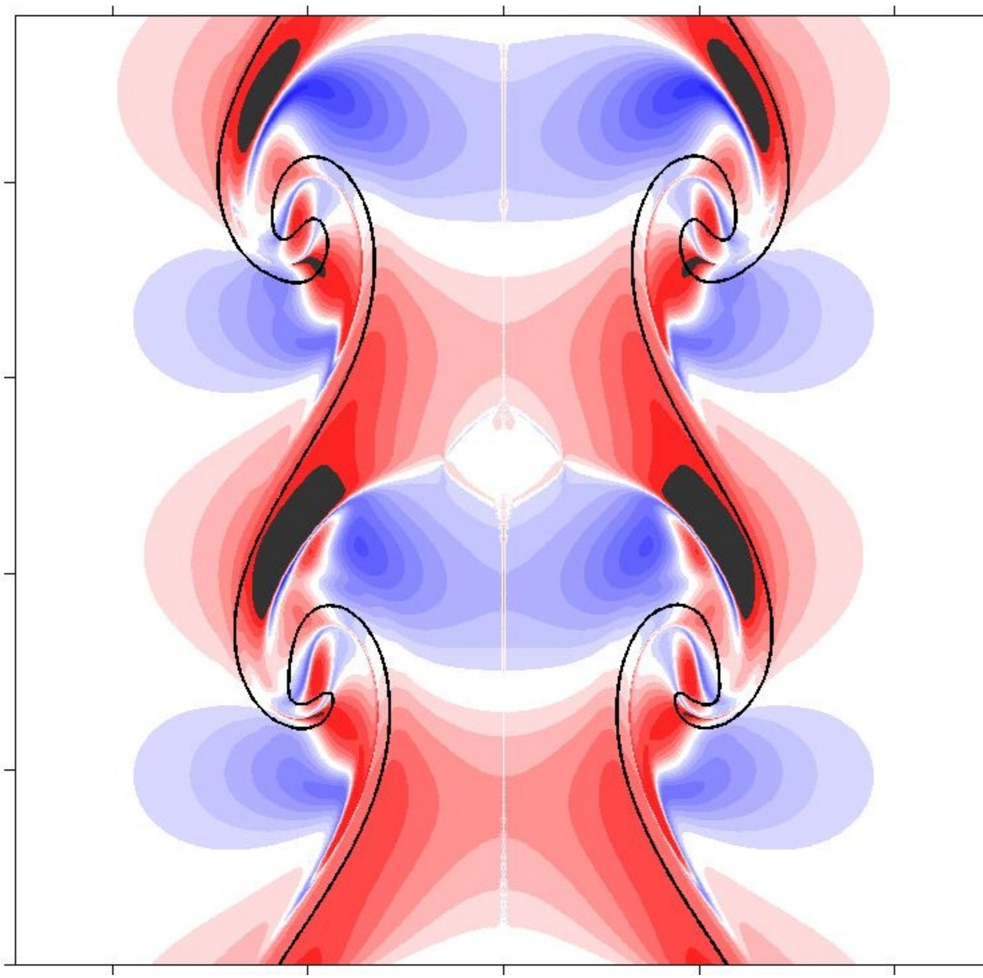

Light jet

t = 4,5

Summary on side jets

Fisrt observation by Monkewitz & Bechert (Album of Fluid Motion - 1988)

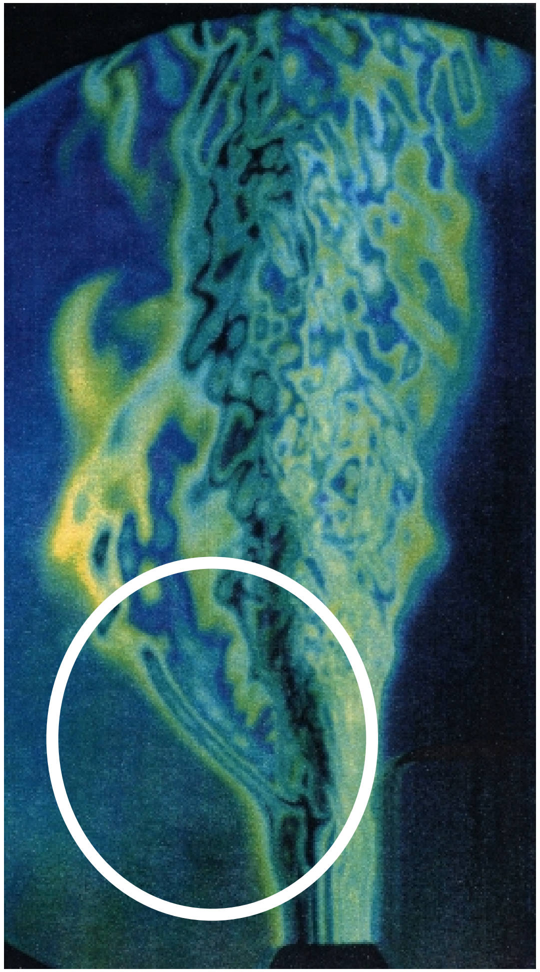

1. The jet is absolutely unstable under a critical density ratio s<0.7,
2. SJ aknowledged within some range of Reynolds number,
3. A shorter route to the mixing transition and a large increase of the mixing rate,
4. SJ recovered in a pulsed homogeneous jet by Monkewitz and Pfizenmaier (1991)
5. From undergoing experiments :
   i. Intemmittent ejection,
   ii. Unsteady number and azymuthal positon,
   iii. Reynolds sensitive azimuthal wavenumber,
   iv. Quasi-steady streamwise position,
   v. Life time of several Primary Mode periods
   vi. How to control SJ and promote mixing

Side ejections on Re = 1000 helium jets from Hermouche, *Institut de Mécanique des Fluides de Toulouse* (1996)

3. *The 2D mixing-layer in the nonlinear regime and the secondary baroclinic instability*

4. *The strain field of 2D low-density jets and the question of side-jets*

   - *The strain fields of low-density jets present a folded layered structure,*
   - *Much higher strain rates may be produced in the baroclinically modified roll-up,*
   - *High strain rates are to be expected « inside » the low-density jet and close to favored leg of the vorticity braid.*
   - *Spontaneous side jets in absolutely unstable low-density jets,*
   - *If understood may help mixing,*

5. *Mass segregation in 2D turbulence and the baroclinic instability of massive vortices*

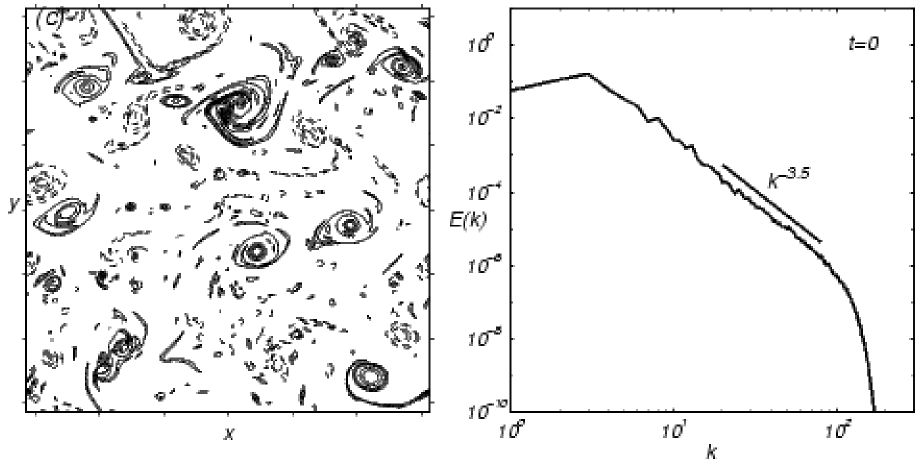

Figure 4.13: Initial vorticity field with solid positive contours and dashed negative ones, increment between contour is $\max(\omega)/2\pi$ and the zero contour is omitted (left); the corresponding energy spectrum (right).

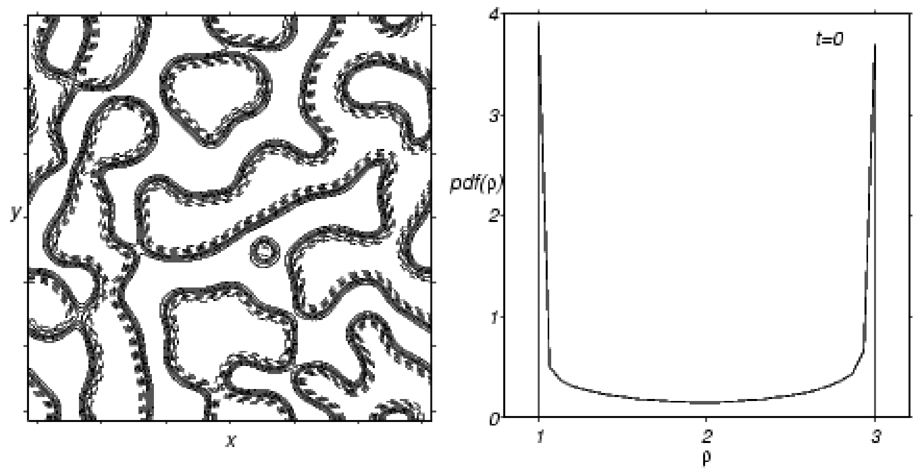

Figure 4.14: Initial density field with solid contours above mean and dashed contours beneath, increment between contour is $\Delta\rho/10$ (left); the corresponding probability density function (right).

Passive scalar 2D turbulence

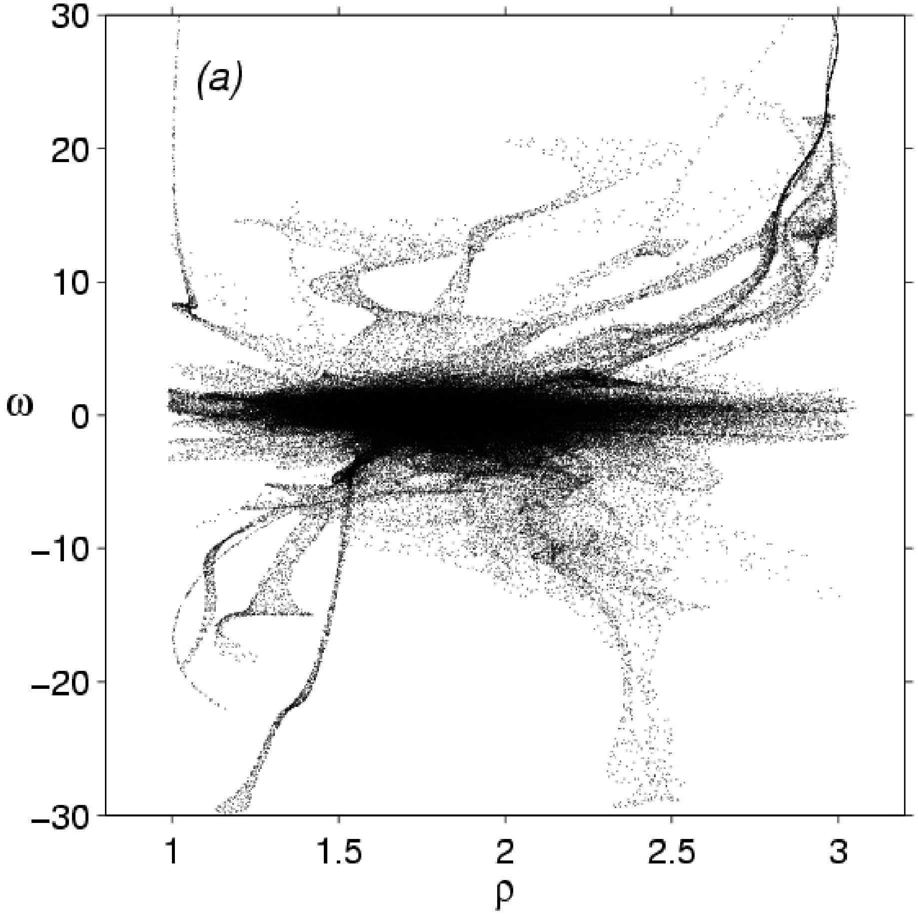

Inhomogeneous 2D turbulence

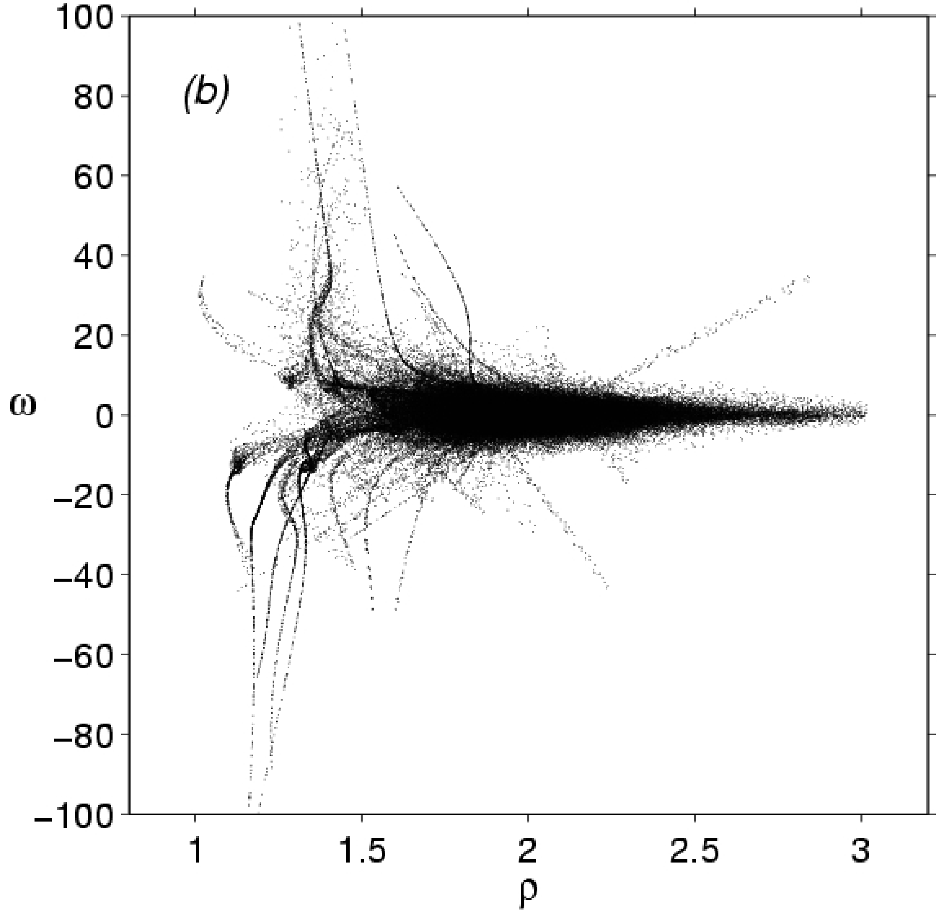

Inspection of an isolated vortex …

The axisymmetric barotropic vortex

A barotropic vortex is a vortex where the pressure depends on density only,

Since $p(\rho)$ *pressure and density gradients are aligned and the barotropic vortex exhibits no baroclinic vorticity sources,*

The axisymmetric vortex with circular isodensity lines (globally advection invariant) is the only barotropic vortex (we found) that is also a steady solution of the Euler (inviscid) equations,

The circular barotropic vortex spreads as a barotropic vortex in the diffusive context,

We study the stability of barotropic vortices with gaussian vorticity and density distributions.

The baroclinic instability mechanism of a perturbated barotropic vortex

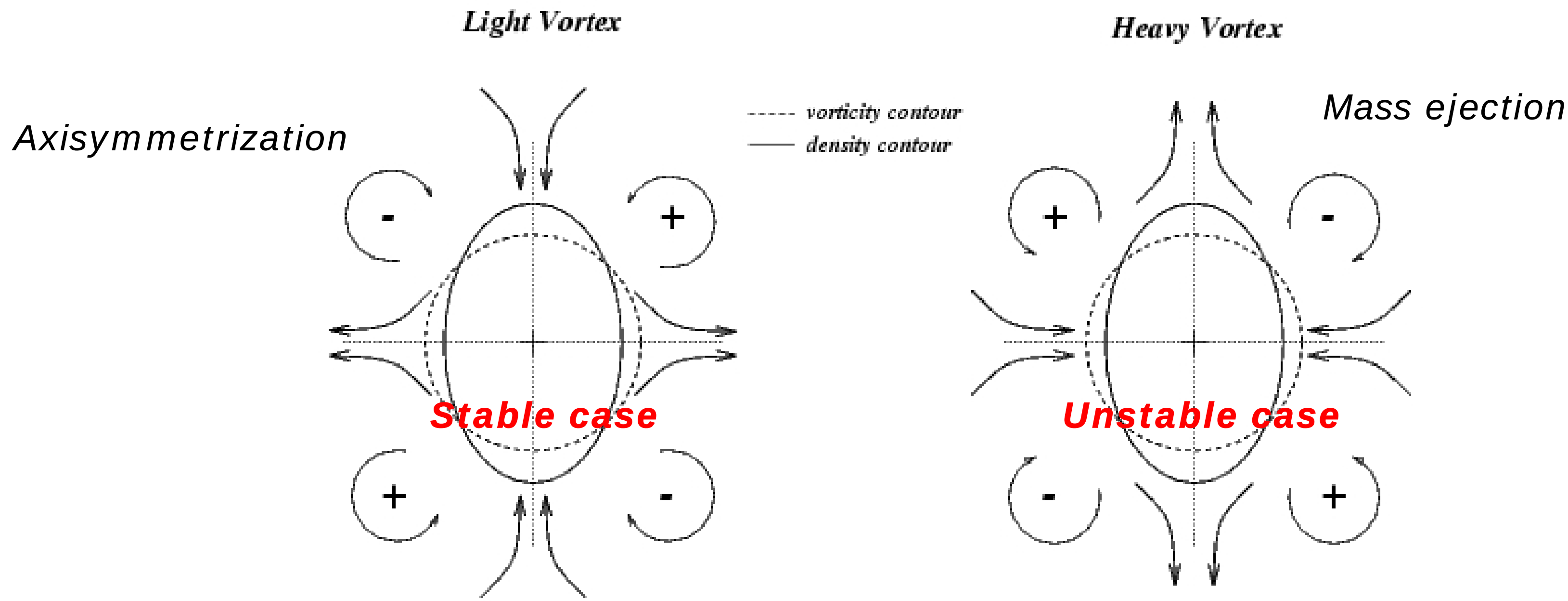

Figure 4.4: Sketch of the baroclinic effects on heavy and light vortices.

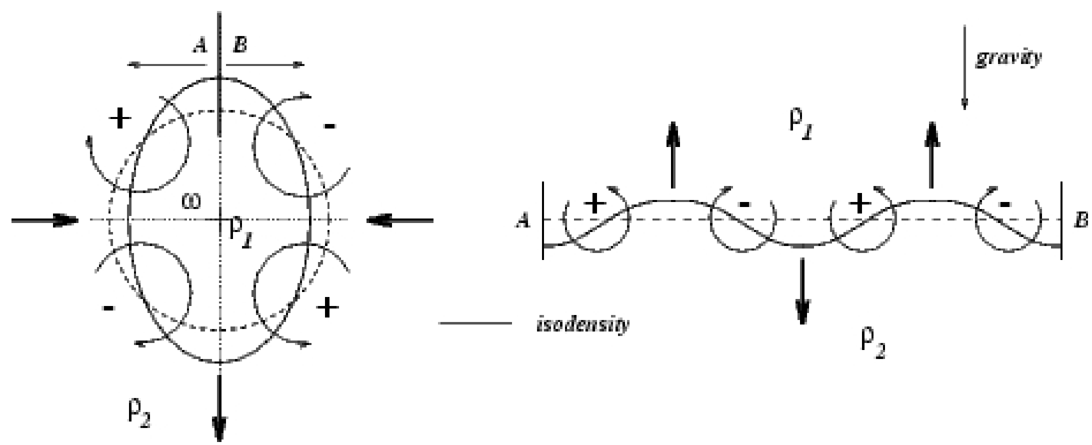

Figure 4.5: Analogy between the heavy vortex and the equivalent unrolled density stratification submitted to a downward gravity field ($\rho_1 > \rho_2$).

Definiton of the base state

$$\Omega(r,\theta) = \frac{\Gamma}{\pi\delta^2}\exp(-\frac{r^2}{\delta^2})$$

$$R = \rho_b + (\rho_c - \rho_b)\exp(-\frac{r^2}{\delta_\rho^2})$$

Density contrast in $[-1, 1]$

$$C_\rho = \frac{\rho_c - \rho_b}{\rho_c + \rho_b}$$

Radius ratio in $[0, \infty[$

$$\varepsilon = \frac{\delta}{\delta_\rho}$$

Linearized Euler equations and normal mode analysis

$$[\hat{u}_r\,,\hat{u}_\theta\,,\hat{p}\,,\hat{\rho}]\,(r,\theta,t) = [iu_r(r), u_\theta(r), p(r), \rho(r)]\exp\left[i\,(m\theta - \omega t)\right]$$

m *Positive integer azimuthal wavenumber*

ω *Complex disturbance phase speed*

Linear stability analysis : main results

Amplification rate in the (density contrast – radius ratio) plane

$$m = 2$$

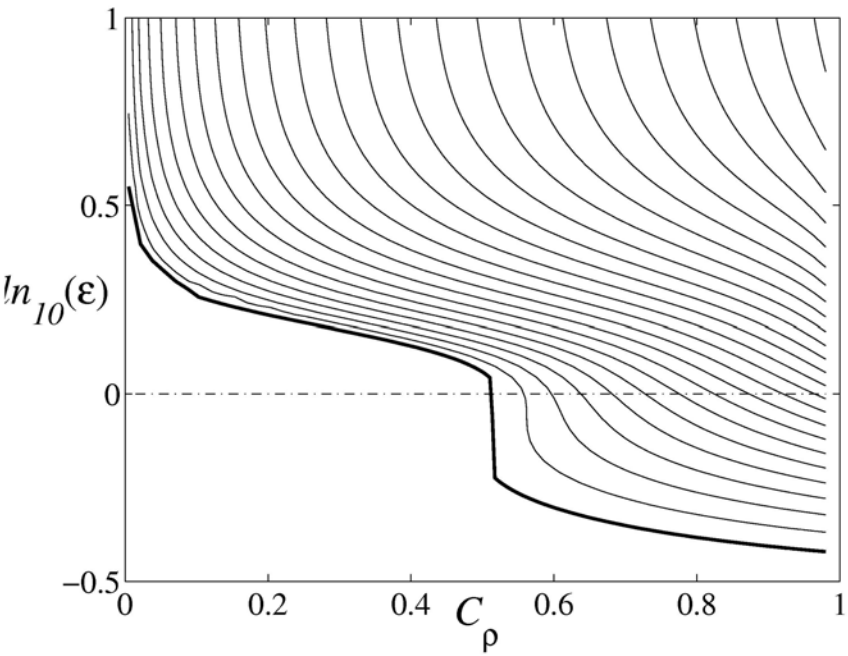

$$m = 3$$

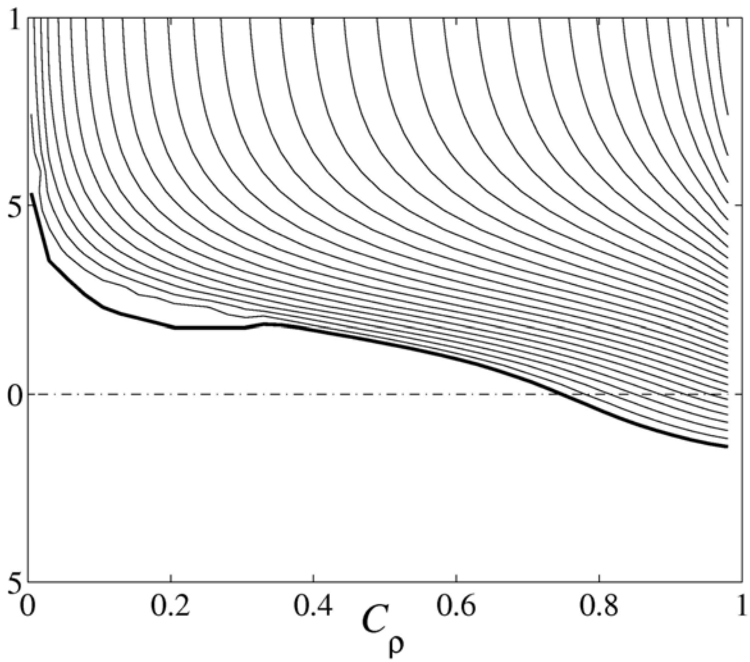

First modes sensitivity to density contrast and radius ratio

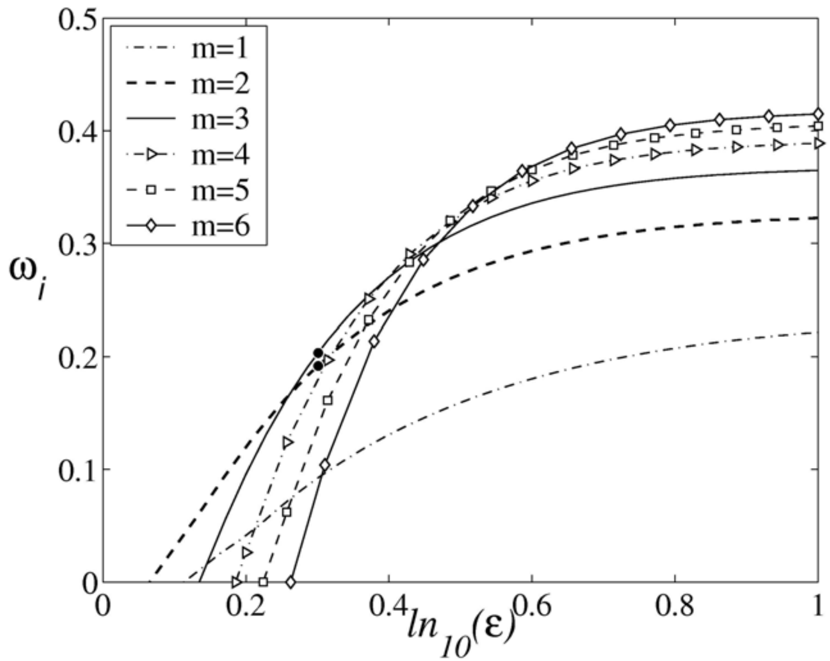

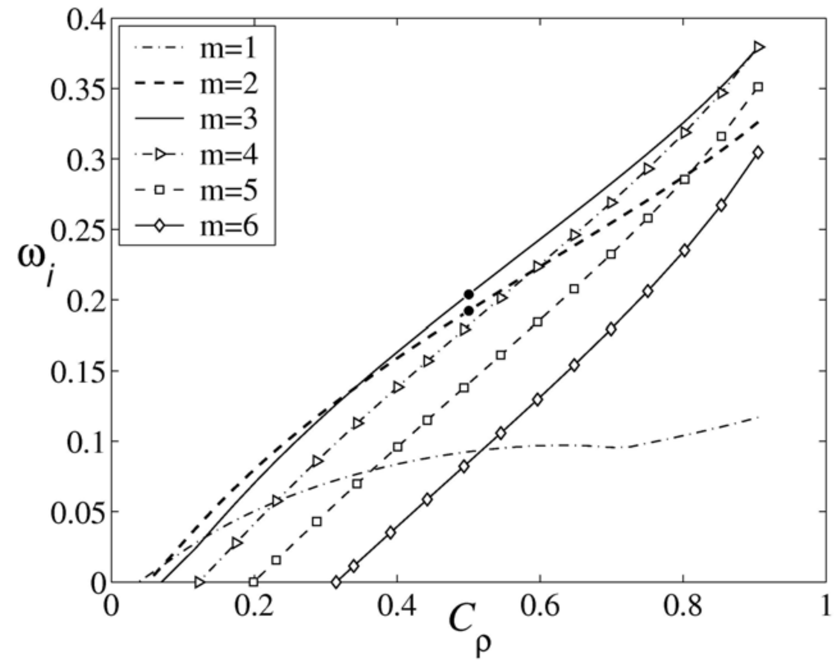

Moderate density constrast

$$C_\rho = 0.5 \text{ or } \rho_c/\rho_b = 3$$

Moderate radius ratio

$$\varepsilon = 2 \text{ or } \delta = 2\delta_\rho$$

Eigen mode perturbation m=3, Cρ = 0.5, ε = 2

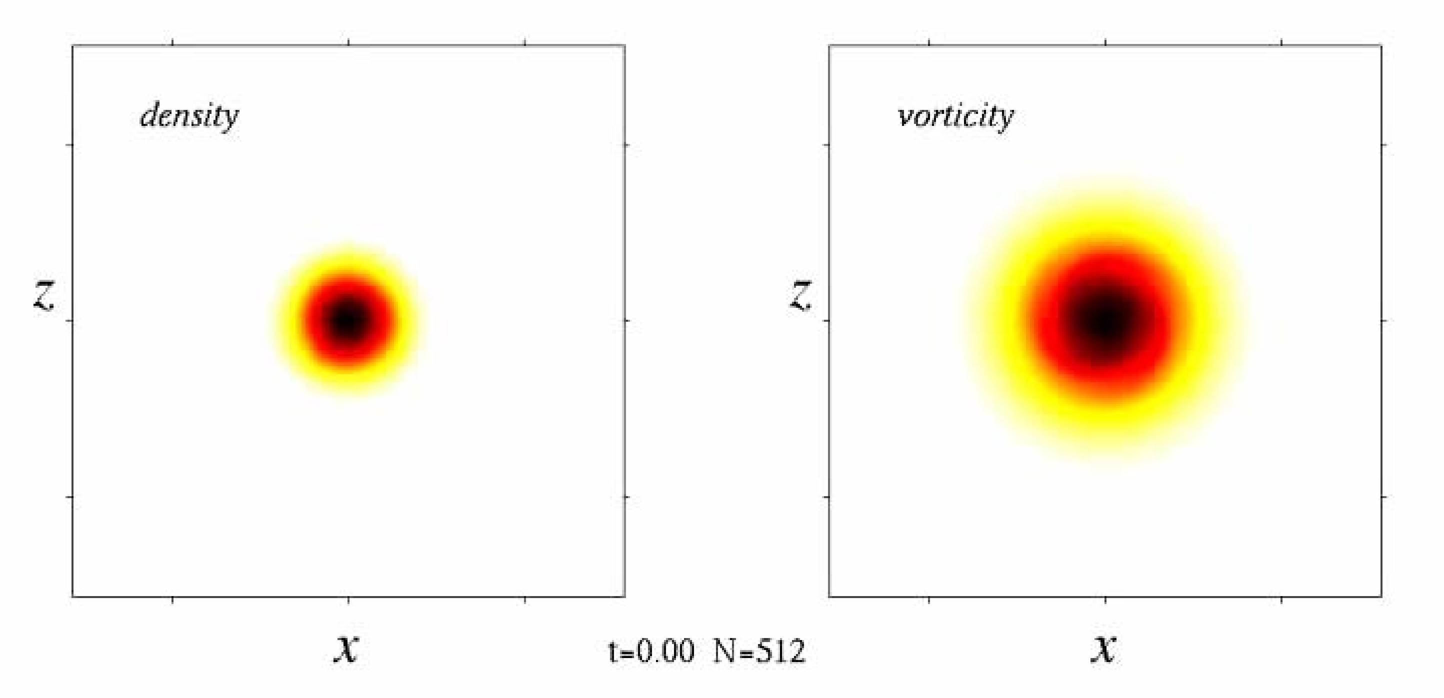

Density radius large amplitude déformation m=3, Cρ = 0.8, ε = 1

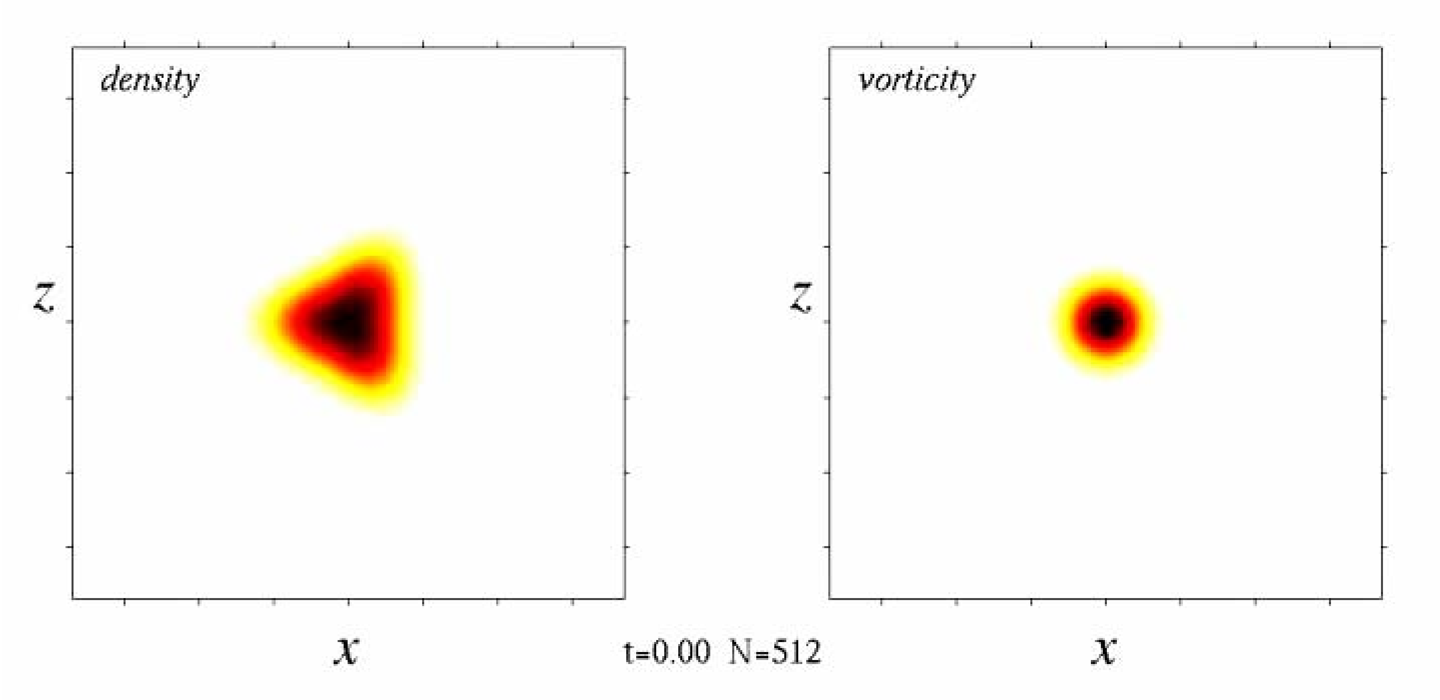

3. *The 2D mixing-layer in the nonlinear regime and the secondary baroclinic instability*
4. *The strain field of 2D light jets the question of side-jets*
5. *Mass segregation in 2D turbulence and the baroclinic instability of massive vortices*

- *Light vortex stable, heavy vortex unstable,*
- *Patches of low-density fluid are robust to vortex interaction : anti-mixing effect on low-density samples*
- *Patches of high-density fluid are ejected from vortex cores and strained lumps of high-density fluid are efficiently smeared out by molecular diffusion : mixing of high-density samples is promoted*
- *Mass segregation by vorticity in 2D inhomogeneous turbulence and asymmetric relaxation of the density pdf.*

Thank you for your attention…

Transition slide

Inviscid incompressible inhomogeneous flows

$$\mathrm{d}_t\rho = 0$$

$$\mathrm{d}_t\mathbf{u} = -g'\mathbf{i}_z - \dot{\mathbf{u}}_r - \frac{1}{\rho}\boldsymbol{\nabla} p$$

$$g' = \frac{g}{\rho_0}(\rho - \rho_{\mathrm{hydro}}) = g\frac{\rho'}{\rho_0} \sim \mathcal{O}(g\,C_\rho)$$

$$\mathbf{a} = \underbrace{\mathrm{d}_t\mathbf{u}}_{\mathrm{II}} + \underbrace{g'\mathbf{i}_z + \dot{\mathbf{u}}_r}_{\mathrm{I}} = -\frac{1}{\rho}\boldsymbol{\nabla} p$$

$$\mathrm{Ba}: \qquad -\frac{1}{\rho}\boldsymbol{\nabla} p \times \boldsymbol{\nabla}\varrho \equiv \mathbf{a} \times \boldsymbol{\nabla}\varrho$$

Scheme of the vorticity generation on the model flow of unstrained counter-rotating vortices

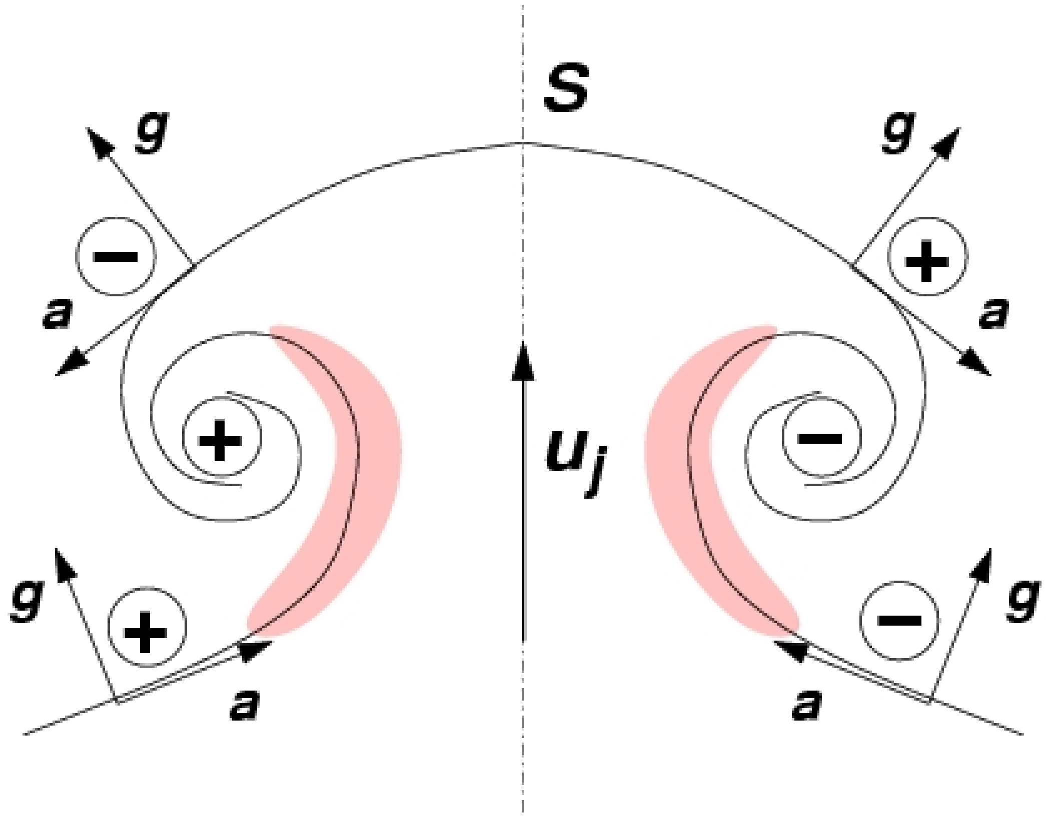

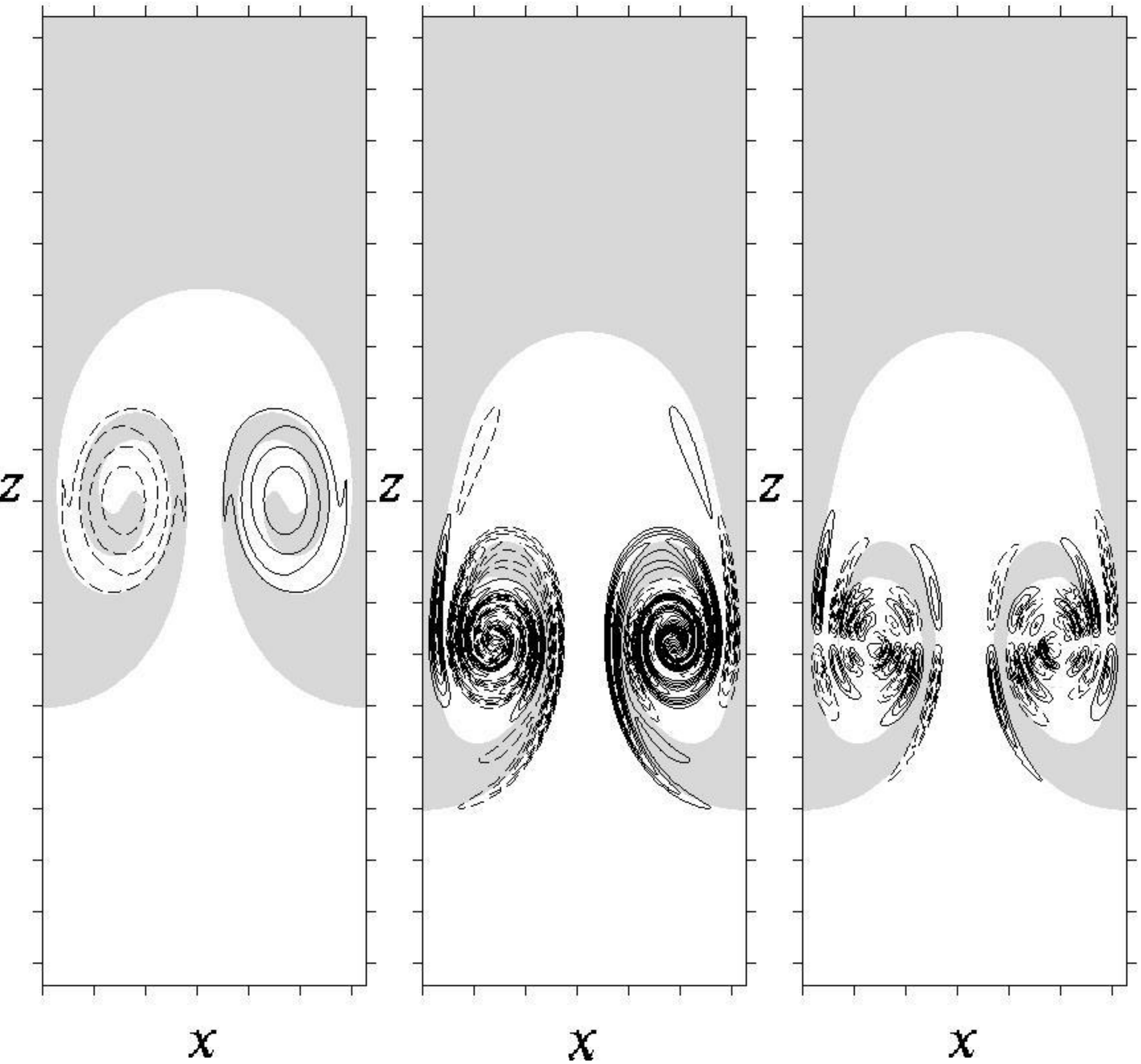

vorticity vorticity Baroclinic torque

- Shift of the vortex centers toward the light side
- Asymmetric entrainment
- A trend expected to be enhanced by the underlynig stretching in braid area

ENSICA

- *Vorticity of the gaussian vortex :*

$$\omega(r,\theta) = \frac{\Gamma}{\pi\delta^2}\exp(-r^2/\delta^2)$$

- *Orthoradial velocity and centripetal acceleration :*

$$\begin{aligned} u_\theta &= [1-\exp(-\frac{r^2}{\delta^2})]\frac{\Gamma}{2\pi\, r} \\ a_r &= -u_\theta^2/r \end{aligned}$$

- *Density field on an elleptic patch :*

$$r_\rho^2(\theta) = r^2[1+(e^{-2}-1)\sin^2\theta]$$

$$\rho(r,\theta) = \rho_e + (\rho_i-\rho_e)\exp(-\frac{r_\rho^2(\theta)}{\delta^2})$$

- *Density gradient vector :*

$$\mathbf{g} = \boldsymbol{\nabla}(\ln\rho) = \begin{cases} g_r = -(1-\frac{\rho_e}{\rho})\frac{2r}{\delta^2}[1+(e^{-2}-1)\sin^2\theta] \\ g_\theta = (1-\frac{\rho_e}{\rho})\frac{r}{\delta^2}(1-e^{-2})\sin(2\theta) \end{cases}$$

- *Baroclinic torque :*

$$b = a_r\, g_\theta = [1-\exp(-\frac{r^2}{\delta^2})]^2\frac{\Gamma^2}{4\pi^2\, r^2\delta^2}(1-e^{-2})\ \frac{\rho_e-\rho}{\rho}\ \sin(2\theta)$$

A set of scales

$$\mathbf{u} \sim u, \quad x, y, z \sim \ell, \quad \pi \sim u^2 \qquad \rho \sim \rho_0, \quad \mathrm{d}\rho \sim \Delta\rho$$

$$\underbrace{\mathrm{d}_t \mathbf{u}}_{\frac{u^2}{\ell}} = -\underbrace{\boldsymbol{\nabla}\pi}_{\frac{u^2}{\ell}} - \underbrace{\pi \boldsymbol{\nabla}\varrho}_{\frac{u^2}{\ell}\frac{\Delta\rho}{\rho_0}} + \underbrace{\nu\Delta\mathbf{u}}_{\nu\frac{u}{\ell^2}}$$

$$\underbrace{\mathrm{d}_t \boldsymbol{\omega}}_{\frac{u^2}{\ell^2}} = \underbrace{(\boldsymbol{\omega}\cdot\boldsymbol{\nabla})\mathbf{u}}_{\frac{u^2}{\ell^2}} - \underbrace{d\,\boldsymbol{\omega}}_{Ma^2\frac{u^2}{\ell}} - \underbrace{\boldsymbol{\nabla}\pi \times \boldsymbol{\nabla}\varrho}_{\frac{u^2}{\ell^2}\frac{\Delta\rho}{\rho_0}} + \underbrace{\nu\Delta\boldsymbol{\omega}}_{\frac{u}{\ell^3}}$$

$$\mathrm{d}_t \varrho = \frac{1}{ReSc}\Delta\varrho = -\frac{1}{C_\rho} d$$

$$\mathrm{d}_t \mathbf{u} = -\boldsymbol{\nabla}\pi - C_\rho \pi \boldsymbol{\nabla}\varrho + \frac{1}{Re}\Delta\mathbf{u}$$

$$C_\rho = \frac{\Delta\rho}{\rho_{\mathrm{mean}}} = \frac{\rho'}{\bar{\rho}}$$

The structure of the 2D low-density jet (with pairing)

Temporal jet s=1/3, Re = UD/ν = 2500

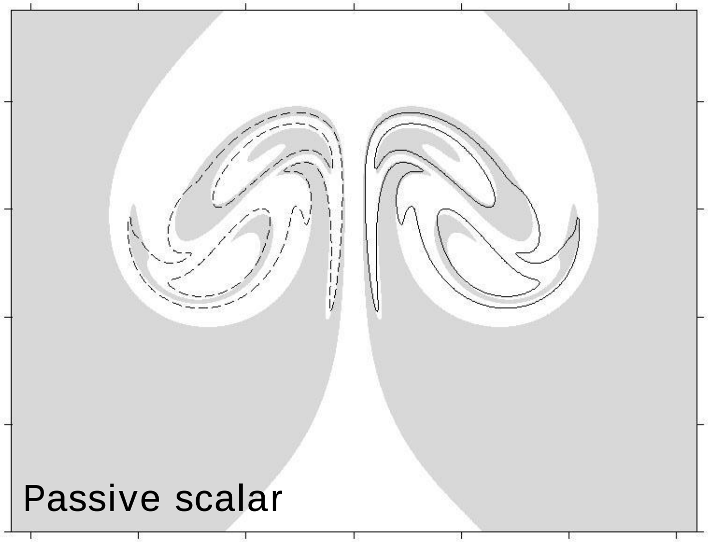

Vorticity

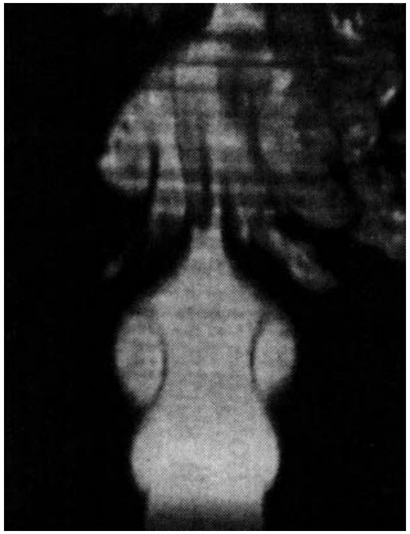

Kyle et Sreenivasan JFM 249 (1993)

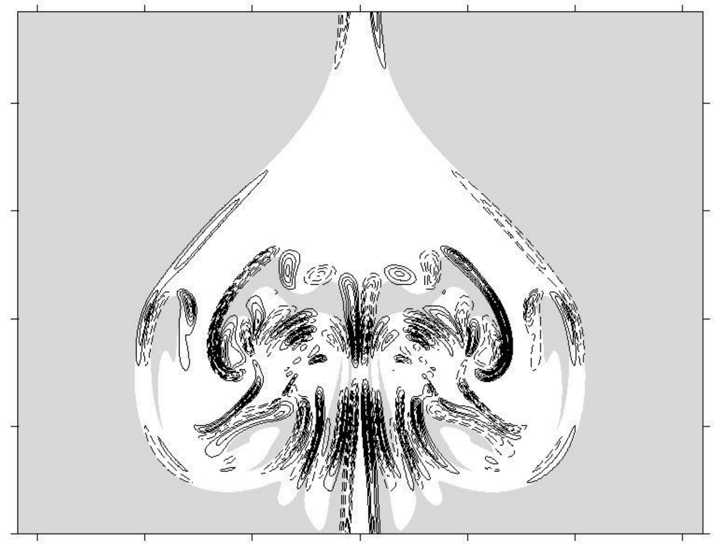

Baroclinic Torque

Temporal jet s=1/3, Re = UD/ν = 2500

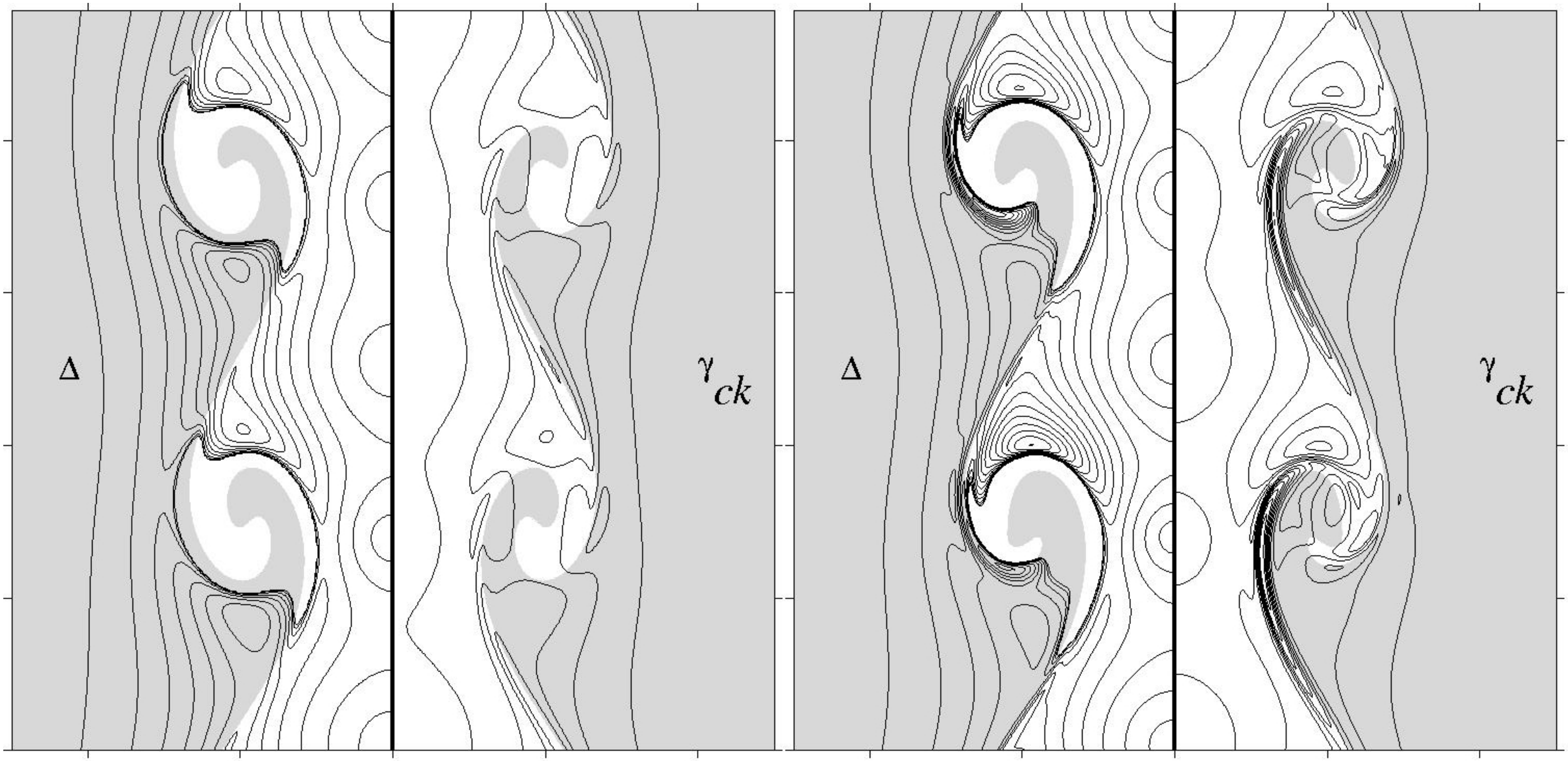

Passive scalar **t = 4,5** *Light jet*

Vortex lourd trois lobes

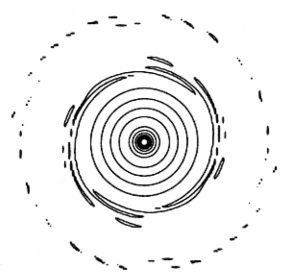

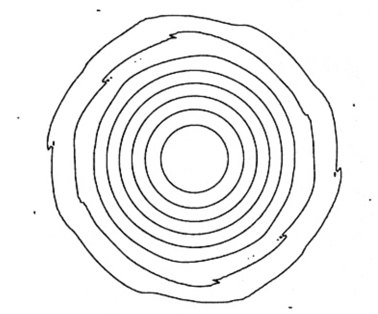

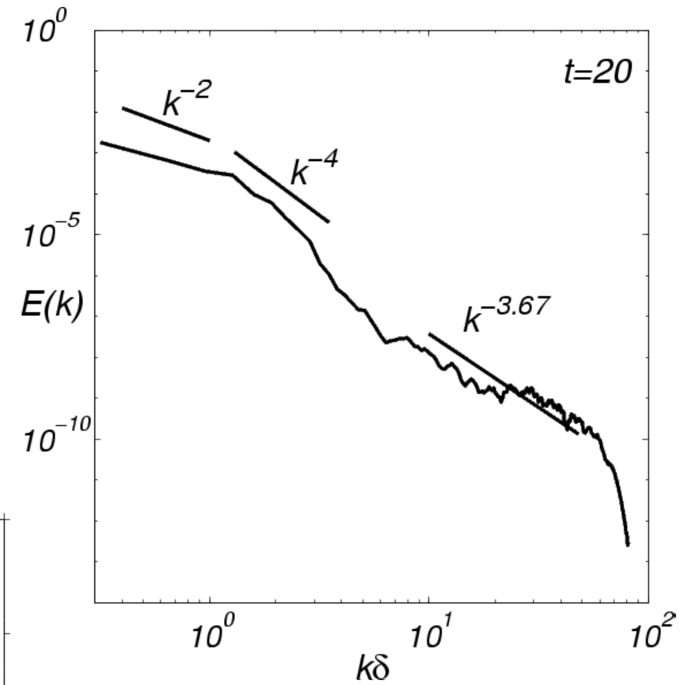

t=20
k^-2
k^-4
k^-3.67
E(k)
10^0
10^-5
10^-10
10^0
10^1
10^2
kδ

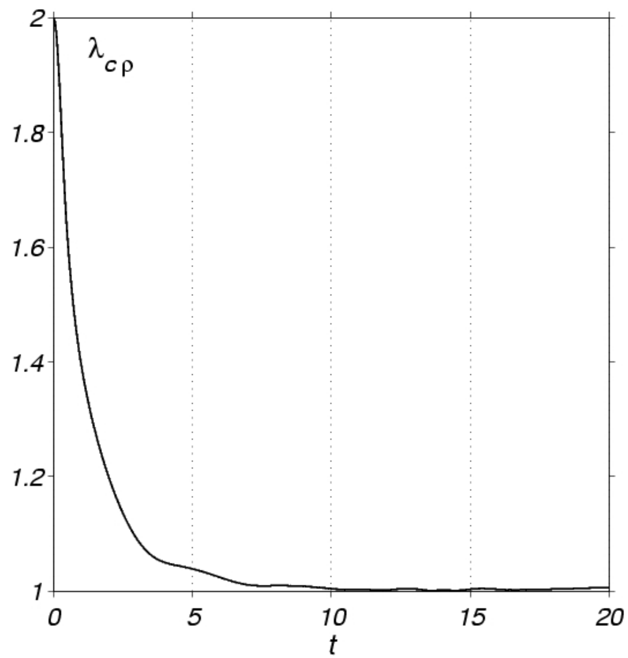

λ_cρ
2
1.8
1.6
1.4
1.2
1
0
5
10
15
20
t

The breakdown of a massive vortex

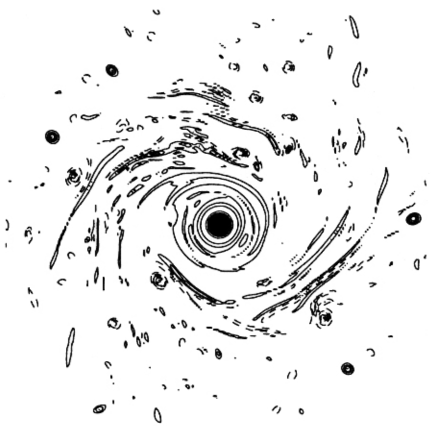

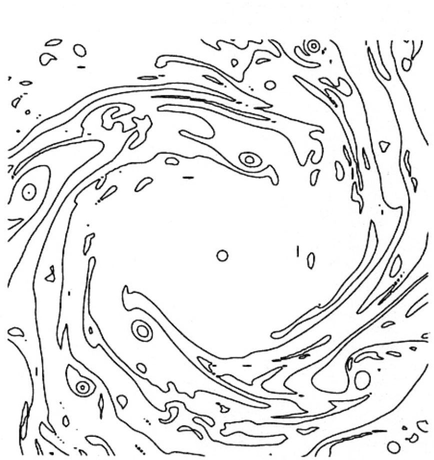

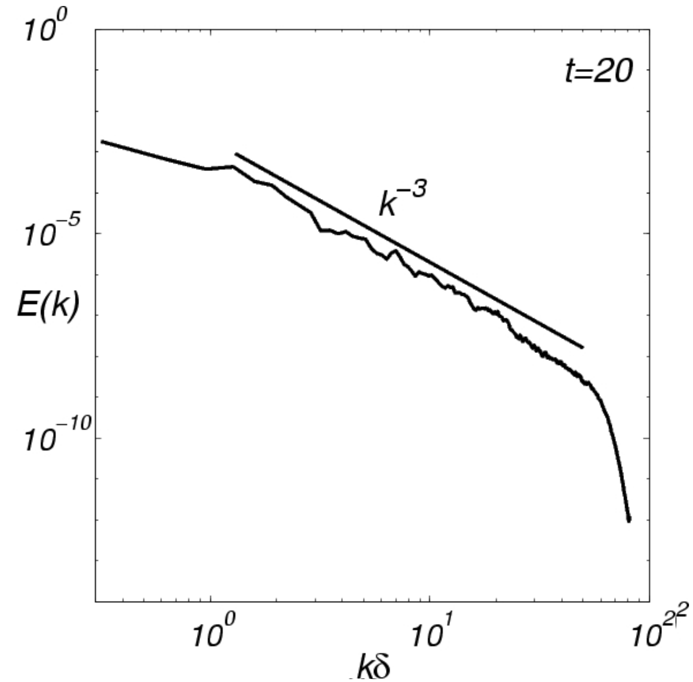

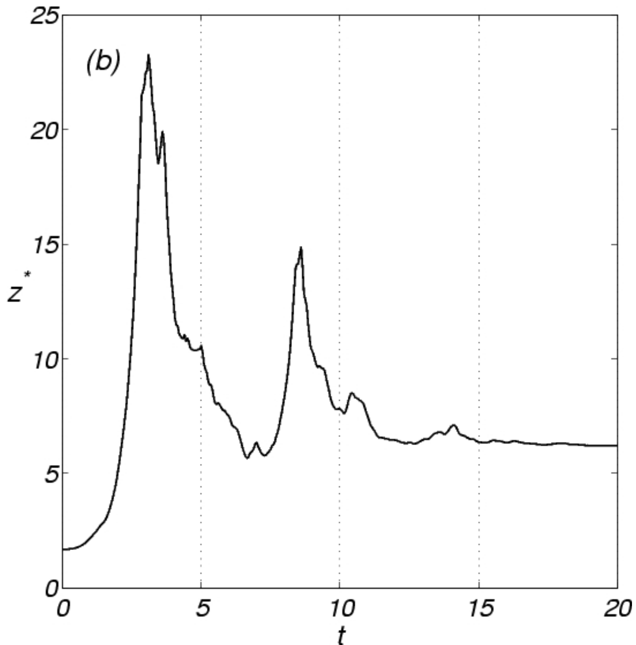

+ *Film with s=10*